

# UC Davis

## UC Davis Previously Published Works

### Title

Regulation of the Ca<sup>2+</sup> Channel CaV1.2 Supports Spatial Memory and Its Flexibility and LTD.

### Permalink

<https://escholarship.org/uc/item/2t4916kr>

### Journal

Journal of Neuroscience, 43(30)

### ISSN

0270-6474

### Authors

Ireton, Kyle E

Xing, Xiaoming

Kim, Karam

et al.

### Publication Date


2023-07-26

### DOI

10.1523/jneurosci.1521-22.2023

Peer reviewed

# Regulation of the Ca<sup>2+</sup> Channel Ca<sub>v</sub>1.2 Supports Spatial Memory and Its Flexibility and LTD

Kyle E. Ireton,<sup>1,2\*</sup> Xiaoming Xing,<sup>1\*</sup> Karam Kim,<sup>1</sup> Justin C. Weiner,<sup>1</sup> Ariel A. Jacobi,<sup>1</sup> Aarushi Grover,<sup>1</sup> Molly Foote,<sup>2</sup> Yusuke Ota,<sup>2</sup> Robert Berman,<sup>2</sup> Timothy Hanks,<sup>2,3</sup> and  Johannes W. Hell<sup>1,2</sup>

<sup>1</sup>Department of Pharmacology, University of California, Davis, California 95616-8636, <sup>2</sup>Center for Neuroscience, University of California, Davis, California 95616-8636, and <sup>3</sup>Department of Neurology, University of California, Davis, California 95616-8636

Widespread release of norepinephrine (NE) throughout the forebrain fosters learning and memory via adrenergic receptor (AR) signaling, but the molecular mechanisms are largely unknown. The  $\beta_2$  AR and its downstream effectors, the trimeric stimulatory G<sub>s</sub>-protein, adenylyl cyclase (AC), and the cAMP-dependent protein kinase A (PKA), form a unique signaling complex with the L-type Ca<sup>2+</sup> channel (LTCC) Ca<sub>v</sub>1.2. Phosphorylation of Ca<sub>v</sub>1.2 by PKA on Ser<sup>1928</sup> is required for the up-regulation of Ca<sup>2+</sup> influx on  $\beta_2$  AR stimulation and long-term potentiation induced by prolonged theta-tetanus (PTT-LTP) but not LTP induced by two 1-s-long 100-Hz tetani. However, the function of Ser<sup>1928</sup> phosphorylation *in vivo* is unknown. Here, we show that S1928A knock-in (KI) mice of both sexes, which lack PTT-LTP, express deficiencies during initial consolidation of spatial memory. Especially striking is the effect of this mutation on cognitive flexibility as tested by reversal learning. Mechanistically, long-term depression (LTD) has been implicated in reversal learning. It is abrogated in male and female S1928A knock-in mice and by  $\beta_2$  AR antagonists and peptides that displace  $\beta_2$  AR from Ca<sub>v</sub>1.2. This work identifies Ca<sub>v</sub>1.2 as a critical molecular locus that regulates synaptic plasticity, spatial memory and its reversal, and LTD.

**Key words:**  $\beta_2$  adrenergic receptor; L-type calcium channels; long-term depression; Morris water maze; norepinephrine; reversal learning

## Significance Statement

We show that phosphorylation of the Ca<sup>2+</sup> channel Ca<sub>v</sub>1.2 on Ser<sup>1928</sup> is important for consolidation of spatial memory and especially its reversal, and long-term depression (LTD). Identification of Ser<sup>1928</sup> as critical for LTD and reversal learning supports the model that LTD underlies flexibility of reference memory.

## Introduction

Learning and memory are fundamental for many functions in daily life spanning from adaptive behaviors all the way to our sense of self. A deeper understanding of the molecular basis by which memories are formed and modified would help illuminate

how our brain executes these functions and could aid the development of new therapeutics for memory disorders. Memory formation is thought to be mediated by modification of synaptic strength through long-term potentiation (LTP) and long-term depression (LTD; Rumpel et al., 2005; Whitlock et al., 2006; Hu et al., 2007; Neves et al., 2008; Kessels and Malinow, 2009; Collingridge et al., 2010; Morris, 2013; Nabavi et al., 2014; Choi et al., 2018; Goto et al., 2021). In particular, hippocampal LTP has been implicated in formation of spatial reference memory in the Morris water maze (MWM; Moser et al., 1998; Vorhees and Williams, 2006; Halt et al., 2012) and LTD is emerging as a potential mechanism for flexibility of previously formed memory in the MWM (Duffy et al., 2008; Nicholls et al., 2008; Dong et al., 2013; Awasthi et al., 2019). Coordinated regulation of LTP and LTD may be an important factor that determines the rate of formation and flexibility of memory within neural circuits, and the balance between memory stability and responsiveness to new situations.

Norepinephrine (NE) is an important neuromodulator that fosters learning and memory, especially in novel or emotionally salient situations (Cahill et al., 1994; Berman and Dudai, 2001;

Received Aug. 2, 2022; revised Apr. 30, 2023; accepted May 15, 2023.

Author contributions: K.E.I., M.F., Y.O., R.B., and J.W.H. designed research; K.E.I., X.X., K.K., A.A.J., and A.G. performed research; J.W.H. contributed unpublished reagents/analytic tools; K.E.I., X.X., K.K., J.C.W., and J.W.H. analyzed data; K.E.I. wrote the first draft of the paper; K.E.I., X.X., T.H., and J.W.H. edited the paper; K.E.I., T.H., and J.W.H. wrote the paper.

This work was supported by National Institutes of Health Grants T32 MH082174, T32 GM007377, and T32 MH112507 (to K.E.I.), T32 MH082174 and T32 GM099608 (to A.A.J.), T32 GM007377 (to J.C.W.), R01NS123050 and RFAAG055357 (to J.W.H.), and R01MH119347 (to Elva D. Diaz and J.W.H.); a Hartwell Foundation grant (T.D.H.), and a University of California (UC) Davis Center for Neuroscience Innovation Award, UC Davis Academic Senate Research Grant; and the UC Davis Behavioral Health Center of Excellence Pilot Grant (T.D.H. and J.W.H.). We thank the Personnel of the UC Davis Mouse Behavioral Assessment Lab, where all behavioral tests were conducted, for their assistance and help with data analysis.

\*K.E.I. and X.X. are co-first authors.

The authors declare no competing financial interests.

Correspondence should be addressed to Timothy Hanks at thanks@ucdavis.edu or Johannes W. Hell at jwhell@ucdavis.edu.

<https://doi.org/10.1523/JNEUROSCI.1521-22.2023>

Copyright © 2023 the authors

Hu et al., 2007; Minzenberg et al., 2008; Carter et al., 2010). Systemic administration of the  $\beta$  AR antagonist propranolol during or after training in the MWM impaired the consolidation of spatial reference memory (S.A. Thomas and Palmiter, 1997; Cahill et al., 2000; Czech et al., 2000; Murchison et al., 2004). Although it is well established that NE acts via  $\alpha$  and  $\beta$  adrenergic receptors (ARs; Caron and Lefkowitz, 1993), the relevant downstream targets that mediate the NE-induced effects in the brain are largely unknown. The  $\beta_2$  AR forms a unique macromolecular signaling complex with the L-type Ca<sup>2+</sup> channel (LTCC) Ca<sub>v</sub>1.2 (Davare et al., 2001). This remarkable complex also contains the trimeric stimulatory G<sub>s</sub>-protein, adenylyl cyclase (AC), and protein kinase A (PKA; Davare et al., 1999; Davare et al., 2001; Hulme et al., 2003; Balijepalli et al., 2006; Hall et al., 2007; Oliveria et al., 2007; Nichols et al., 2010; Marshall et al., 2011; Murphy et al., 2014). Furthermore,  $\beta_2$  AR signaling potently upregulates Ca<sub>v</sub>1.2 activity in neurons by inducing its phosphorylation at Ser<sup>1928</sup> via PKA in a highly localized manner (Davare et al., 2001; Patriarchi et al., 2016; Qian et al., 2017). These findings suggest that Ca<sub>v</sub>1.2 is a key target for NE signaling. Mutations and variations in the Ca<sub>v</sub>1.2-encoding CACNA1C gene have also been identified as risk factors for various neuropsychiatric disorders in which impaired learning is often a comorbidity, including schizophrenia, bipolar disease, major depression, attention deficit hyperactive disorder, and autism spectrum disorders (Splawski et al., 2004; Ferreira et al., 2008; Green et al., 2010; Nyegaard et al., 2010; Bhat et al., 2012).

Ca<sup>2+</sup> signaling via LTCCs and especially Ca<sub>v</sub>1.2 is important for LTP, learning, and memory (Grover and Teyler, 1990; Moosmang et al., 2005; White et al., 2008). Ca<sub>v</sub>1.2 accounts for ~80% of LTCCs in the brain (Hell et al., 1993; Sinnegger-Brauns et al., 2004) and is concentrated in hippocampal dendritic spines (Hell et al., 1996; Davare et al., 2001). Ca<sub>v</sub>1.2 is essential for LTP that is induced by prolonged theta rhythm tetanus (PTT; 90- to 180-s-long tetanus of 5–10 Hz; Patriarchi et al., 2016; Qian et al., 2017), an activity pattern of the brain that is important for learning (Jensen and Lisman, 2005; Mizuseki et al., 2009). PTT-LTP requires simultaneous stimulation of the  $\beta_2$  AR during the PTT (Qian et al., 2012), phosphorylation of Ca<sub>v</sub>1.2 on Ser<sup>1928</sup> by PKA (Qian et al., 2017), and the interaction of the  $\beta_2$  AR with Ca<sub>v</sub>1.2 (Patriarchi et al., 2016; Man et al., 2020b). Collectively, these findings strongly suggest that regulation of Ca<sub>v</sub>1.2 by NE-triggered Ser<sup>1928</sup> phosphorylation is a major mechanism of NE signaling in the brain. However, the *in vivo* relevance of Ser<sup>1928</sup> phosphorylation is not known.

Identification of molecular pathways that regulate both synaptic strength and the formation and flexibility of memory, could provide a leverage point to uncover the neural mechanisms that connect synaptic plasticity to learning. Because S1928A knock-in (KI) mice completely lack PTT-LTP, we hypothesized that S1928A KI mice would exhibit impairments in memory-related behavior tasks. We report that the acquisition and consolidation of spatial reference memory are impaired. Especially striking are deficits in reversal of spatial memory in the MWM. Surprisingly, but consistent with the deficits in reversal learning, S1928A KI mice failed to display any LTD in acute hippocampal slices. Furthermore, acute inhibition of the  $\beta_2$  AR by corresponding antagonists and acute disruption of the  $\beta_2$  AR–Ca<sub>v</sub>1.2 interaction by a membrane-permeant peptide mimicking the binding site for the  $\beta_2$  AR on Ca<sub>v</sub>1.2 also impaired LTD. Accordingly, the main effect of abrogating regulation of Ca<sub>v</sub>1.2 by NE may be a change in the

rate of spatial memory consolidation and its reversal because of impaired LTP and LTD, respectively.

## Materials and Methods

### Mice

All animal procedures followed NIH guidelines and were approved by the University of California (UC) Davis Institutional Animal Care and Use Committee (IACUC). Mice were housed on a 12/12 h light/dark cycle, with light on from 7 A.M. to 7 P.M. Litter-matched Ca<sub>v</sub>1.2 wild-type (WT) and S1928A KI mice were bred from heterozygous S1928A mice, with a 50% B6J/50% 129Sv background (Lemke et al., 2008; Patriarchi et al., 2016; Qian et al., 2017). Mice were kept in group housing with three to five mice of mixed genotype to randomize their distribution across housing conditions. All experiments were conducted between 9 A.M. and 4 P.M. and were performed with age-matched and litter-matched wild-type (WT) and S1928A KI mice of mixed sex (evenly distributed gender ratios; mice within a cohort were not more than three weeks apart) at an age of three to six months. The experimenter was blind to the genotype.

### Open field test

Mice were placed into an open arena measuring 26 × 26 × 39 cm with opaque walls, to explore freely for 30 min. Photocells tracked total movement by IR beam-breaking, in 1 cm units. TruScan analysis software produced a readout report in 5-min time bins of movement, speed, and time in the center of the arena (TruScan Photobeam Sensor–E63-22; Coulbourn Instruments).

### Y-Maze novel arm recognition

Mice were placed into an opaque three-arm Y-shaped maze and allowed to explore two arms for an initial period of 10 min. The third arm was made unavailable by means of an opaque separator. After initial exploration, mice were removed and placed back into their home cage, for an interval of either 2 min or 4 h. The opaque arm separator was removed during the interval, and the maze floor wiped down with 70% Ethanol to remove odor cues from previous exploration. After the interval elapsed, the mice were returned to the same starting arm position as in the initial period and allowed to explore for 5' more. During this period, mouse movement and entry into the novel and familiar arms opposite the start arm were tracked by Anymaze software. Afterward, the discrimination index (DI) for exploration time in the novel versus familiar arm was calculated [DI = Time<sub>Novel</sub> / (Time<sub>Novel</sub> + Time<sub>Familiar</sub>)].

### Novel object location recognition

Mice were habituated to an empty arena measuring 50 × 50 cm for 30 min, over 3 consecutive days. On day 4, mice were placed into the same arena but with the addition of two identical objects on the side of the arena opposite to the start position. Mice were allowed to freely explore and investigate the objects for 15 min, then returned to their home cages for 2 h. Afterward, mice were returned to the arena once more with one of the two identical objects now moved to the opposite side of the box (novel object location). The right and left objects were pseudorandomly selected to be moved, to counterbalance any preference of right versus left. Mice were once again allowed to freely explore and investigate both objects, with exploration bouts counted when the mice entered a 1.5-cm radial circle zone around either of the objects, with their nose oriented toward the object. The frequency and cumulative time of bouts were tracked and quantified by Noldus Ethovision software. DI was calculated for the frequency of exploration bouts and time spent investigating for the novel location object versus familiar object location [DI = Bouts<sub>Novel</sub> / (Bouts<sub>Novel</sub> + Bouts<sub>Familiar</sub>)].

### Morris water maze

Mice were trained to find the location of a hidden, submerged platform in a pool of opaque water with navigation cues located on curtains around the pool. Training trials occurred four times per day per mouse for 7 consecutive days. Mice were released from a different cardinal direction at the edge of the pool for each trial, varied in a pseudorandom order for counterbalancing. Mice were introduced to the curtained

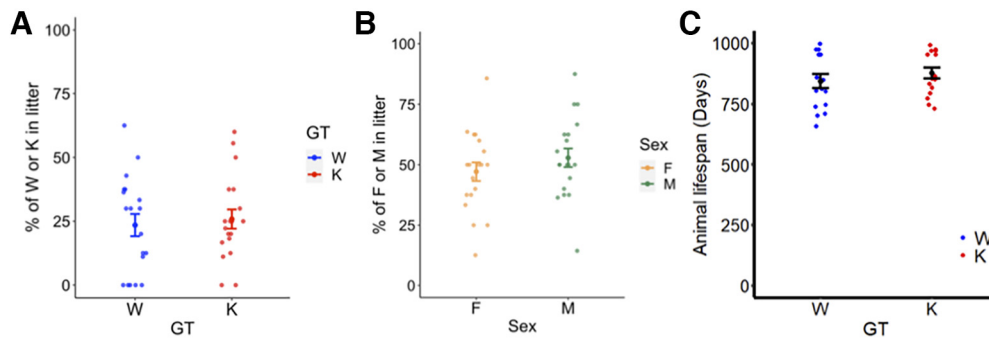


**Figure 1.** Birth ratio for genotype and sex from heterozygous WT/S1928A KI breeders and life expectations. **A**, Offspring genotype from heterozygous WT/S1928A KI breeders follows expected Mendelian distribution (WT/WT:  $n = 38$ , 26.4%; WT/KI:  $n = 68$ , 47.2%; KI/KI:  $n = 38$ , 26.4). **B**, Offspring from heterozygous WT/S1928A KI breeders have normal sex distribution (WT/WT: F = 21, 55% and M = 17, 45%; WT/KI: F = 31, 46% and M = 37, 54%; KI/KI: F = 17, 45% and M = 21, 55%). **C**, Life expectation of homozygous WT/WT and KI/KI mice from heterozygous breeders was comparable [WT:  $n = 16$ ; KI/KI:  $n = 16$ ; black bars show group mean  $\pm$  SEM; difference in means (DM) =  $-33.7$ , 95% confidence interval (95% CI) =  $(-107.3, 39.8)$ ,  $p = 0.355$ ,  $t$  test].

testing arena by two different routes depending on starting position in the pool (one route for two starting positions, each), and allowed up to 60 s to locate the platform with 10 s to acclimate on the platform after locating it. If mice failed to reach the platform after 60 s, they were guided gently by hand, and allowed 10 s to acclimate. Probe tests occurred  $\sim 24$  h after the most recent training trials before training on days 4 (probe test 1, P1) and 7 (P2) and 10 d after the last training day (P3) with no additional training in between. During probe tests, the platform was removed from the pool and mice allowed to freely explore the pool for 60 s. Mice were brought into the testing area by a different route from those used during training trials, and released at the point furthest from the platform location (diagonally opposite, i.e., SW corner), which was also not used as a start location during any training trials. For analysis, the pool was divided into four equal sized quadrants, with the platform goal zone also demarcated in the center of the “NE” quadrant, and the remaining quadrants designated by cardinal directions as “NW,” “SW,” and “SE” Time elapsed to first enter the platform goal zone, dwell time in each quadrant zone, and total distance and speed of travel were all tracked and quantified by Anymaze software.

Reversal training began the day after P3 (i.e., day 18 overall). Training occurred as previously described, with the platform moved to the center of the “SW” quadrant, which was opposite to the original platform location, in all trials. The reversal probe test (P4) was conducted  $\sim 24$  h following the final training trial. Mice were brought into the testing area by again a different route from those used in any previous training trials and probe tests, and released from the edge of the pool at the point furthest from reversal platform location (i.e., “NE” corner), which also was not used as a start location during any training trials or previous probe tests. Analysis was conducted in the same fashion as in the previous probes, but with the reversal platform zone additionally demarcated and performance parameters tracked respectively in Anymaze.

#### Long-term potentiation and depression

Field recordings were conducted in acute hippocampal slices prepared from six-week to four-month-old S1928A KI mice and WT, as previously described (Qian et al., 2012, 2017; Patriarchi et al., 2016). Briefly, after sectioning and a 1- to 2-h recovery time, brain slices were transferred to the recording chamber and perfused (2 ml/min) at 30°C with artificial cerebrospinal fluid (ACSF, without GABA receptor antagonists; in mM: 127 NaCl, 26 NaHCO<sub>2</sub>, 1.2 KH<sub>2</sub>PO<sub>4</sub>, 1.9 KCl, 2.2 CaCl<sub>2</sub>, 1 MgSO<sub>4</sub>, and 10 D-glucose, 290–300 mOsm/kg) saturated with 95% O<sub>2</sub>-5% CO<sub>2</sub> (final pH 7.3). Field EPSPs (fEPSPs) in the hippocampal CA1 region were evoked every 15 s by stimulating the Schaffer collateral pathway with a bipolar tungsten electrode and recorded with a glass electrode filled with ACSF. Signals were amplified with an Axopatch 2B amplifier, digitized with a Digidata 1320A, and recorded with Clampex 9 (Molecular Devices). The test stimulus strength was set to result in 50% of maximal response. LTP was induced by two tetani (100 Hz for 1 s) that were 10 s apart. LTD was induced by a train of pulses with a

frequency of 1 Hz lasting either 30 min (1800 pulses) in slices prepared in the morning (i.e., at the start of the mice’s inactive phase) from six- to eight-week-old mice or 15 min in slices prepared in the late afternoon (i.e., at the start of the mice’s active phase) from three- to four-month-old mice. The baseline was determined by the average of fEPSP initial slopes from the 5-min period immediately before the tetanus. The level and significance of LTP and LTD was determined by the average of fEPSP initial slopes from the 5-min period between 55 and 60 min (LTP), 70 and 75 min (1800 pulse LTD), or 45 and 50 min (900 pulse LTD) after the start of the tetanus. When indicated, slices were preincubated for 30 min with 10  $\mu$ M of an N-terminally myristoylated peptide mimicking the binding site of the  $\beta_2$  AR on CaV1.2 (myrPep2; WT sequence: myr-LGRRASFHLECLKRQKNQGG) or a scrambled version of it (myrPep2Scr; scrambled sequence: Myr-GGQNSFAGLRLERCLHKRQK) as described previously (Patriarchi et al., 2016).

#### Statistical analyses

All data are represented as mean  $\pm$  SEM. Where indicated, data were analyzed by Welch two-sample, two-sided  $t$  test ( $t$  test), ANOVA, with repeated measures as appropriate (ANOVA), or ANOVA followed by Tukey’s test for *post hoc* analysis (indicated in legends). Analyses were calculated in R version 4.0 on Windows, using the RStudio IDE. Trends ( $p < 0.1$ ) are indicated by the symbol #.

#### Data availability

Raw data tables show quantified measures of performance for individual mice in the different behavioral tasks, and are represented in the text and figures where appropriate as mean  $\pm$  SEM. Raw data will be made available on request to qualified researchers.

## Results

Initial work did not find any significant differences in the general development, locomotion, or motor learning of S1928A KI mice versus WT (Lemke et al., 2008). Because CaV1.2 triggers our heart beat it is important to note that S1928A KI mice had normal  $\beta$  adrenergic receptor-mediated upregulation of the cardiac CaV1.2 and of the heart beat under various conditions (Lemke et al., 2008), which we confirmed more recently (Qian et al., 2017). In retrospect, the lack of any obvious cardiac phenotype in S1928A KI mice is surprising because our subsequent work showed that in neurons upregulation of CaV1.2 by the  $\beta_2$  AR is completely absent in S1928A KI mice (Qian et al., 2017). It is now clear that in the heart the main mechanism is mediated by phosphorylation of Rad, which as an interactor of the cardiac CaV1.2, but it is not readily detectable in hippocampal neurons (Liu et al., 2020; Man et al., 2020a). These findings minimize potential confounding cardiovascular effects in our study on the

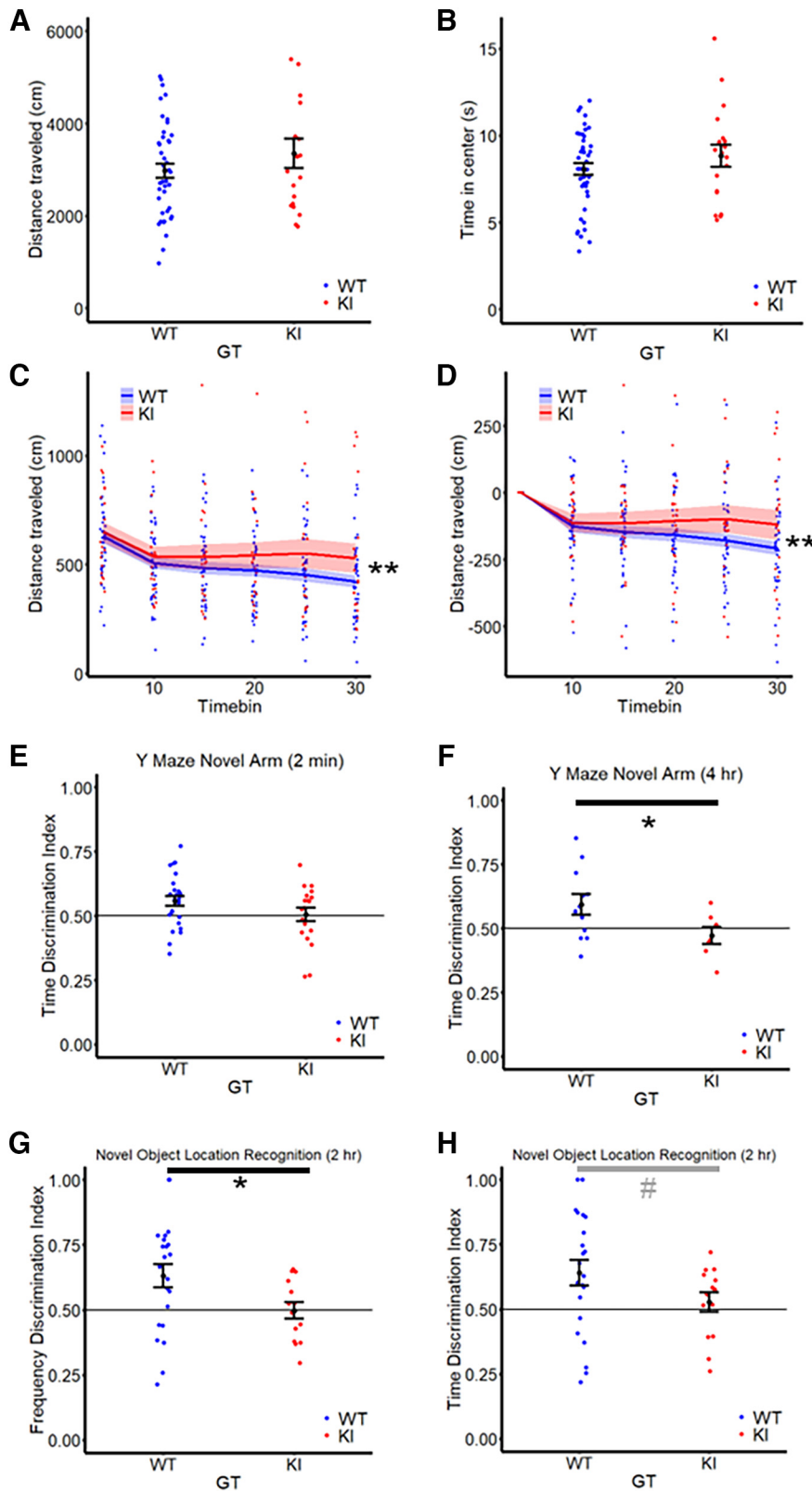


**Figure 2.** Habituation and familiarity memory were impaired in S1928A KI mice. Open field behavior and memory in the novel arm and novel object location were analyzed in three- to six-month-old WT and litter-matched S1928A KI mice. **A**, Total locomotion in the open field over 30 min [WT  $n = 43$ ; S1928A  $n = 19$ ; black bars show group mean  $\pm$  SEM; difference in means (DM) =  $-376.1$ , 95% confidence interval (95% CI) =  $(-1104.8, 352.6)$ ,  $p = 0.299$ ,  $t$  test]. **B**, Total time in center of open field over 30 min [DM =  $-0.77$ , 95% CI =  $(-2.25, 0.71)$ ,  $p = 0.297$ ,  $t$  test]. **C**, Locomotion in the open field, per 5-min cumulative time bins (mean, solid line; SEM, shaded region;  $p < 0.01$  GT  $\times$  Time, ANOVA). **D**, Change in individual locomotion in the open field from the first 5-min time bin ( $p < 0.01$  GT  $\times$  Time, ANOVA). **E**, Discrimination index (DI) for novel arm dwell time in Y-maze familiarity test, with 2-min interval [WT  $n = 12$ ; S1928A  $n = 7$ ; black puncta and bars

role of the Ca<sub>v</sub>1.2 S1928 phosphorylation in the brain. Furthermore, we found that the birth ratio of homozygous S1928A KI and WT mice from heterozygous breeders followed the expected Mendelian distribution of 25% homozygous KI and WT and 50% heterozygous offspring (Fig. 1A). The sex distribution was also normal in our offspring from heterozygous breeders (Fig. 1B). In addition, we followed the life expectation in one cohort, which was also comparable between S1928A KI and WT mice (Fig. 1C).

### S1928A KI mice display reduced habituation to a novel context in an open field test

In the open field mice show initially high locomotive activity, which substantially declines over a 10- to 30-min period (Grailhe et al., 1999; Malleret et al., 1999; Zhuang et al., 2001). This habituation reflects, among other mental processes, acquisition of spatial familiarity, an initial step of spatial recognition learning. We assessed habituation of WT and KI mice by determining the reduction in movement from beginning to end of 30-min-long sessions in 5-min time bins in an open field arena. The two genotypes did not significantly differ with respect to total distance traveled or time spent in the center over 30-min periods in the open field, suggesting no difference in baseline locomotion (Fig. 2A, B). Habituation was evident for both groups (Fig. 2C,D). The main within-subject effect by time for all mice combined was significant ( $p < 0.001$ ; ANOVA). The mixed genotype  $\times$  time interaction was significant ( $p = 0.005$ ; Fig. 2C), suggesting differences in habituation between groups. KI mice traveled more as a group later in the session, suggestive of less habituation. Directly comparing the difference in movement between the first 5-min time bin and subsequent time bins for each individual mouse revealed diminished habituation to the novel arena in S1928A KI versus WT mice, with less of a decrease in movement between bins for KI individuals (Fig. 2D).

←

show group mean  $\pm$  SEM; black mid-line shows 0.5; DM = 0.054, 95% CI =  $(-0.012, 0.119)$ ,  $p = 0.11$ ,  $t$  test]. **F**, DI for novel arm dwell time in Y-maze familiarity test, with 4-h interval [DM = 0.12, 95% CI =  $(0.011, 0.232)$ ,  $*p = 0.033$ ,  $t$  test]. **G**, DI for exploration frequency in Novel Object Location familiarity test [WT  $n = 22$ ; S1928A  $n = 14$ ; black bars show group mean  $\pm$  SEM; black mid-line shows 0.5; DM = 0.14, 95% CI =  $(0.020, 0.246)$ ,  $*p = 0.02$ ,  $t$  test]. **H**, DI for exploration time in Novel Object Location familiarity test [DM = 0.12, 95% CI =  $(-0.01, 0.52)$ ,  $\#p = 0.07$ ,  $t$  test].

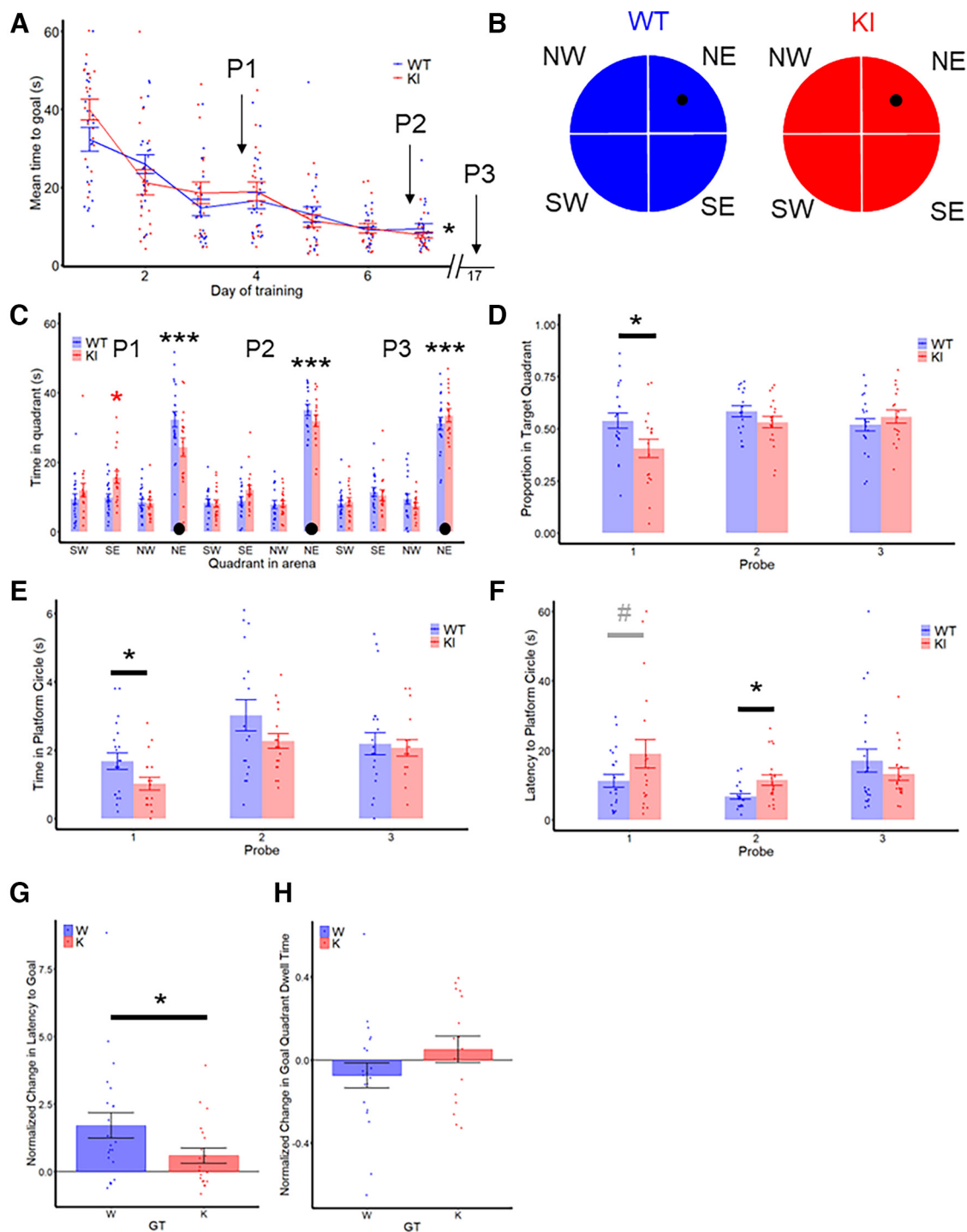


**Figure 3.** S1928A KI mice were impaired in early but not late consolidation of reference memory in the Morris water maze. Learning and memory was analyzed in three- to six-month-old WT and litter-matched S1928A KI mice. **A**, Mean (solid lines)  $\pm$  SEM (whiskers) of time to reach platform in grouped training trials, across days (WT,  $n = 25$ ; S1928A,  $n = 23$ ,  $*p = 0.050$  GT  $\times$  Trial, ANOVA). Arrows indicate timepoints for probe testing (P1, before training on day 4; P2, before training on day 7; P3, on day 17). **B**, Diagram of quadrant scheme for scoring pool behavior, with platform position marked in black (NE quadrant). Naming scheme for quadrants matches subsequent panel (WT, blue; S1928A, red). **C**, Time spent in each quadrant during probe testing. Bars show group mean  $\pm$  SEM (error bars). Asterisks indicate significance for ANOVA *post hoc* Tukey's test against other quadrants, per group and probe test (black circles mark goal quadrant;  $***p < 0.001$ ,  $*p < 0.05$ ; red asterisks correspond to tests for S1928A group only). **D**, Percent time dwelling in target quadrant during probe tests. Bars show group mean and error bars  $\pm$  SEM [P1: DM = 0.14, 95% CI = (0.017, 0.250),  $*p = 0.026$ ,  $t$  test; P2: DM = 0.04, 95% CI = (−0.02, 0.12),  $p = 0.18$ ,  $t$  test; P3: DM = 0.04, 95% CI = (−0.12, 0.05),  $p = 0.38$ ,  $t$  test]. **E**, Time dwelling in target platform zone during probe tests. Bars show group mean and error bars  $\pm$  SEM [P1: DM = 0.66, 95% CI = (0.04, 1.27),  $*p = 0.037$ ,  $t$  test; P2: DM = 0.75, 95% CI = (−0.29, 1.79),  $p = 0.15$ ,  $t$  test; P3: DM = 0.13, 95% CI = (−0.68, 0.94),  $p = 0.75$ , Welch  $t$  test]. **F**, Latency to reach target platform in probe tests. Bars show group mean and error bars  $\pm$  SEM [P1: DM = −8.25, 95% CI = (−17.92, 1.42),  $\#p = 0.09$ ,  $t$  test; P2: DM = 3.67, 95% CI = (−7.27, −0.09),  $*p = 0.045$ ,  $t$  test; P3: DM = 5.02, 95% CI = (−2.81, 12.57),  $p = 0.20$ ,  $t$  test]. **G**, Means  $\pm$  SEM of normalized changes for each individual mouse in latency to first reach goal between acquisition probes P2 and P3 ( $t$  test,  $*p = 0.04$ ). **H**, Means  $\pm$  SEM of normalized changes for each individual mouse in dwell time in goal quadrant between acquisition probes P2 and P3 ( $t$  test,  $*p = 0.016$ ).

The mixed genotype  $\times$  time interaction was significant for the difference in movement between time bins ( $p = 0.005$ ; Fig. 2D). Accordingly, KI mice require more time than WT to habituate to the open field context, consistent with the notion that KI mice might be impaired with respect to short-term memory processes underlying spatial familiarity and recognition.

### S1928A KI mice fail to display single trial spatial familiarity memory

Spatial memory was more directly assessed using the novel arm assay, in a three-arm Y-maze. Mice were released at the end of one arm, and allowed to explore it and one neighboring arm for 15 min. The third arm was concealed from view by a door. After exploration, mice were returned to their home cage for 2 min in one set of experiments and 4 h in another. The door to the third arm was removed before mice were again placed at the end of the initial start arm and allowed to freely explore all three arms of the maze for 5 min. The fraction of time spent in the novel arm divided by combined time in the two nonstarting arms constitutes the discrimination index (DI) as a metric for preference of the novel arm (Kraeuter et al., 2019). The DI of WT versus KI mice was close to being significant after a 2-min delay ( $p = 0.11$ ; Fig. 2E). When the delay was extended to 4 h to make this task more difficult, the difference in DI for WT versus KI mice became larger and significant ( $p = 0.033$ ; Fig. 2F). Accordingly, spatial memory is impaired in KI mice after long and likely also short delays.

Spatial memory was further interrogated in a novel object location recognition assay. Mice were habituated to an open arena for 20 min/d for 3 consecutive days. On day 4, two identical objects were placed on the same side of the arena at an equal distance from the starting location of the mice. After free exploration for 15 min, the mice were returned to their home cages for a 2-h delay interval and then re-introduced to the arena with one of the two identical objects moved to the opposite side. KI mice showed a significant reduction in DI of exploration bout frequency for the object in the novel location ( $p = 0.022$ ; Fig. 2G) and near significant reduction in cumulative exploration time versus WT ( $p = 0.07$ ; Fig. 2H).

Collectively, the differences in open field habituation, DIs in novel arm, and DIs in novel location assays indicate that spatial memory is impaired in KI mice. Based on the different timescales of these experiments, this impairment appears to be true for both short-term (minutes) and long-term (hours) memory processes.

### Spatial learning in the MWM is impaired in S1928A mice

Spatial learning, its rate of consolidation, and its subsequent reversal were analyzed in the MWM task (Morris, 1984; Vorhees and Williams, 2006). A total of 23 WT and 20 litter-matched S1928A KI mice, three to six months old, underwent MWM training. Average training trial latency to reach the platform for each day decreased across all days in both genotypes (main within-subject effect by Day for all mice combined was  $p < 0.001$ ; ANOVA), and there was not a main effect by GT ( $p = 0.38$ ). However, there was a threshold Genotype (GT)  $\times$  Day interaction ( $p = 0.050$ ), which suggests differences in spatial learning trajectories by GT as a group (Fig. 3A,B).

The platform was removed before probe trials for testing memory, which were conducted on test days before any training

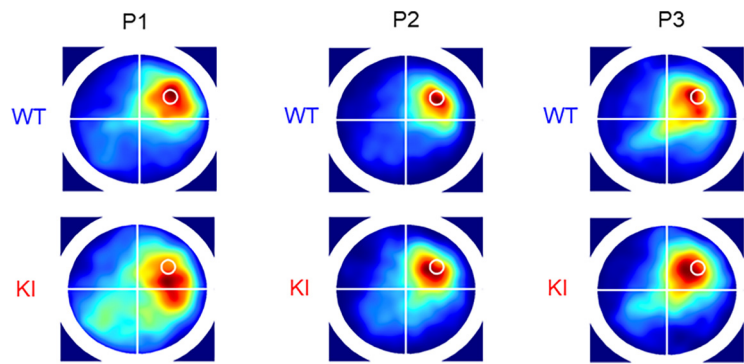


**Figure 4.** Heat maps of individual position density during probe tests in the Morris water maze. White outline shows pool circumference and white lines divisions between quadrants for scoring. Small white circle in NE quadrant shows location of platform zone. Hotter colors indicate greater density of position throughout probe test and cooler colors less density.

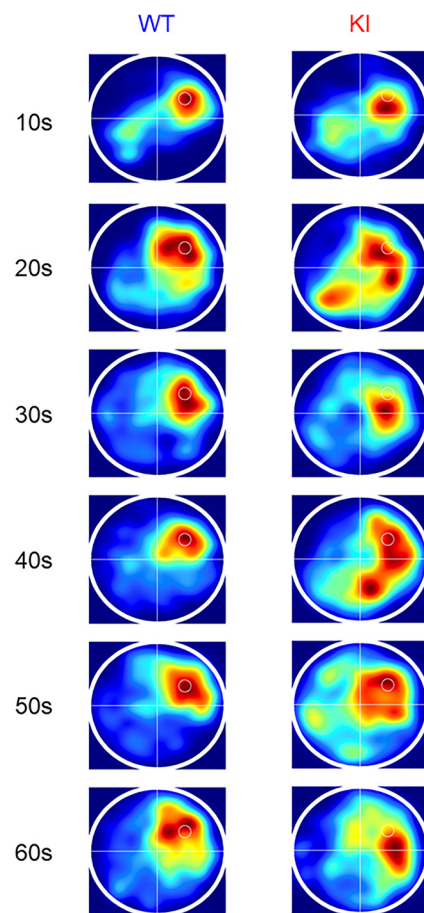


**Figure 5.** S1928A mice showed impaired early consolidation of reference memory across time bins, during first probe test in the Morris water maze. Position density heatmaps for genotype groups during the early consolidation probe test before training on day 4 (P1). Maps are arranged from top to bottom as 10-s time bins in series throughout the 60-s probe, and labeled as such. WT are on the left, and KI on the right. Hotter colors (reds) represent greater density of individual positions across each time bin, and cooler colors (blues) represent lesser density.

trials took place on those days. During the probe test P1 on day 4, dwell time was significantly greater for the goal quadrant over all other quadrants in both genotypes, indicating general spatial memory (WT NE-SW  $p < 0.001$ , NE-NW  $p < 0.001$ , NE-SE  $p < 0.001$ ; S1928A NE-SW  $p < 0.001$ , NE-NW  $p < 0.001$ , NE-SE

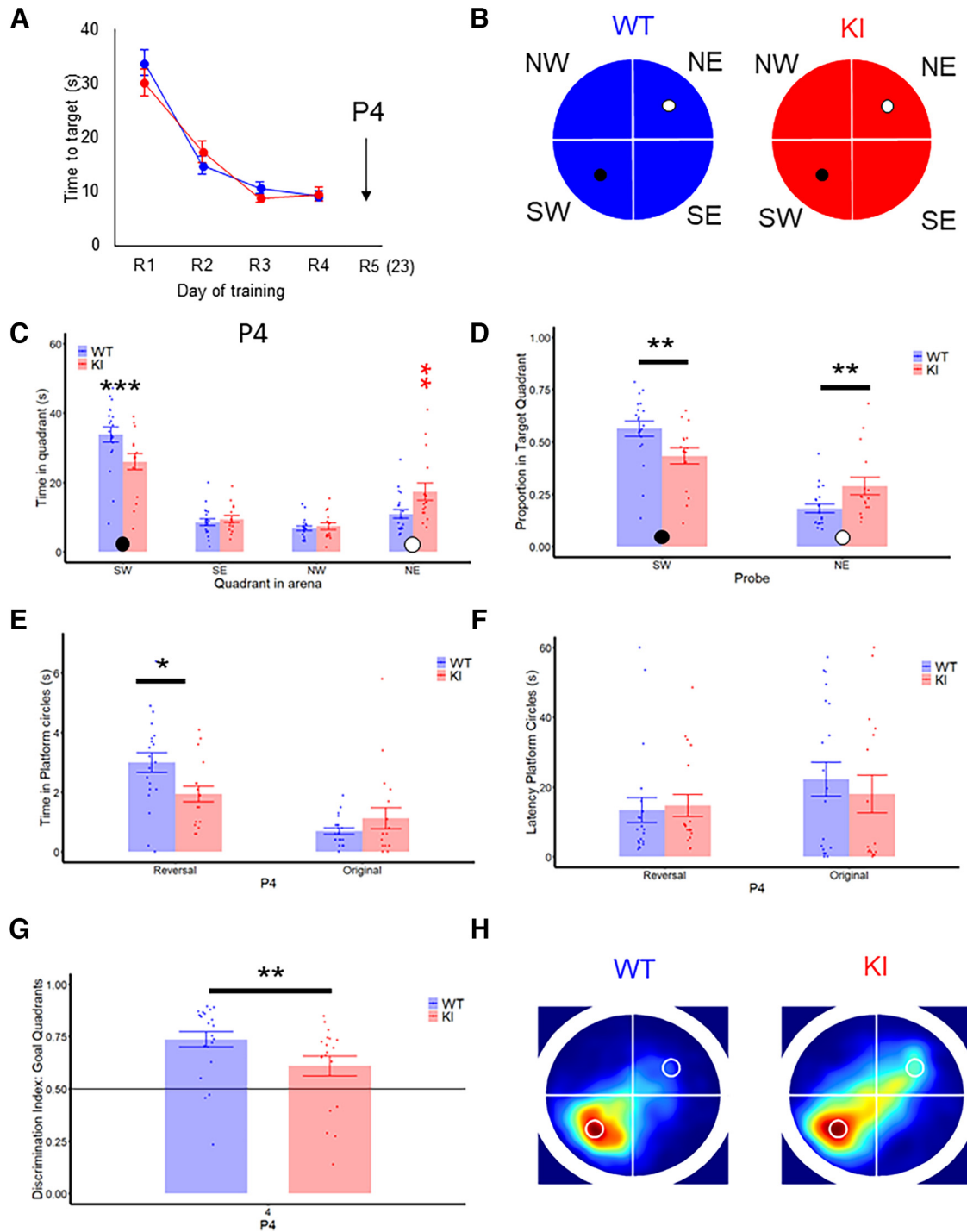


**Figure 6.** S1928A KI mice were impaired in reversal reference memory in the Morris water maze. **A**, Mean  $\pm$  SEM of time to reach platform in grouped reversal training trials, across days (WT,  $n = 25$ ; S1928A,  $n = 23$ ). Arrows indicate time point for reversal probe test (P4, on day R5, day 23 overall). **B**, Diagram of quadrant scheme for scoring pool behavior, with new reversal platform position marked in black (SW quadrant), and original goal location marked in white (NE quadrant; WT, blue; S1928A, red). **C**, Time spent in each quadrant during reversal probe test. Bars show group mean and error bars  $\pm$  SEM. Stars indicate significance for ANOVA with *post hoc* Tukey's test against all other quadrants, per group (black and white circles indicate reversal and original goal quadrant, respectively; \*\*\* $p < 0.001$ , \*\* $p < 0.01$ , red asterisks correspond to S1928A group only). **D**, Proportion time dwelling in reversal and original target quadrants during probe tests. Bars show group mean and error bars  $\pm$  SEM. Black bars show group comparisons [black and white circles indicate reversal and original goal quadrant, respectively; SW: DM = 7.84, 95% CI = (1.32, 14.33),  $p = 0.020$ ,  $t$  test; NE: DM = 6.41, 95% CI = (−12.15, −0.67),  $p = 0.030$ ,  $t$  test]. **E**, Dwell time in platform circle zones during reversal probe test. Bars show group mean and error bars  $\pm$  SEM [reversal: DM = 1.11, 95% CI = (0.27, 1.95),  $p = 0.01$ ,  $t$  test; original: DM = 0.39, 95% CI = (−1.12, 0.34),  $p = 0.28$ ,  $t$  test]. **F**, Latency to reach target platform zones in reversal probe test. Bars show group mean and error bars  $\pm$  SEM (reversal: DM = 0.36, 95% CI = (−8.79, 9.52),  $p = 0.93$ ,  $t$  test; original: DM = 2.16, 95% CI = (−12.73, 17.04),  $p = 0.77$ ,  $t$  test). **G**, DI for dwell time in reversal versus original target quadrant zones. Dots and error bars show group mean  $\pm$  SEM; black line shows hypothetical mean of 0.5 [DM = 0.13, 95% CI = (0.01, 0.24),  $p = 0.009$ ,  $t$  test]. **H**, Heat maps of individual position density during reversal probe test. White outline shows pool circumference, and white lines show divisions between quadrants for scoring. Small white circles show locations of reversal platform zone (SW), and original platform zone (NE). Hotter colors indicate greater density of position throughout probe test and cooler colors less density.



$p = 0.012$ ; Fig. 3C). However, compared with WT, KI mice showed a significant decrease in dwell time for the goal quadrant ( $p = 0.026$ ; Fig. 3D) and precise platform location ( $p = 0.037$ ; Fig. 3E); the increase in latency to first reach the platform zone was close to being significant ( $p = 0.09$ ; Fig. 3F). Position density heatmaps for P1 revealed a directly overlapping hotspot for the platform zone in WT, but was off center for KI mice (Fig. 4). Areas of longest dwell times of KI mice were closest to the original platform location during the first 10-s time bin, but this focus degraded with respect to how narrow and close the search areas were to the original platform location in all subsequent time bins for KI mice, when degradation was minimal for WT mice (Fig. 5). Thus, KI mice appeared to be less certain about the platform location than WT mice. Collectively, these data suggest less accuracy of fine-grained spatial reference memory in KI versus WT mice during the early phase of memory consolidation. Accordingly, spatial memory is weaker, perhaps because the rate of its consolidation is slower in the KI mice at this phase of learning.

During P2 on day 7, after three more full days of training, dwell time was again significantly greater for the goal quadrant over the others for both genotypes (WT NE-SW  $p < 0.001$ , NE-NW  $p < 0.001$ , NE-SE  $p < 0.001$ ; S1928A NE-SW  $p < 0.001$ , NE-NW  $p < 0.001$ , NE-SE  $p < 0.001$ ; Fig. 3C). Similarly to P1, KI mice exhibited a significant increase in the latency to first reach the platform zone ( $p = 0.045$ ) versus WT (Fig. 3F) and a tendency toward a decrease in dwell time for the goal quadrant ( $p = 0.18$ ; Fig. 3D) and the platform circle area ( $p = 0.15$ ; Fig. 3E), but the latter two effects did not reach significance. The position density heatmap during P2 revealed directly overlapping hotspots for the platform zone in WT as well as KI mice, indicative of refined and increased behavioral expression of reference memory in both GTs after further training (Fig. 4). These data suggest that prolonged training increased the accuracy of spatial reference memory in both genotypes to the point that performance became more similar.

Remote memory consolidation was assessed 10 d after the final day of training in P3. Both genotypes maintained a significant preference for the goal quadrant over all others (WT: NE-SW  $p < 0.001$ , NE-NW  $p < 0.001$ , NE-SE  $p < 0.001$ ; S1928A: NE-SW  $p < 0.001$ , NE-NW  $p < 0.001$ , NE-SE  $p < 0.001$ ; Fig. 3C), which was at this time point comparable for both genotypes ( $p = 0.38$ ; Fig. 3D) as were dwell times in the precise target zone ( $p = 0.75$ ; Fig. 2E) and latency to first reach it ( $p = 0.20$ ; Fig. 3F). The heatmap of position density revealed a precisely overlapping hotspot with the platform zone for WT as well as KI mice (Fig. 4). Accordingly, both genotypes demonstrated high retention of reference memory in remote consolidation.

In summary, S1928A KI mice exhibited a notably slower rate of consolidation of reference memory as seen during early probe tests P1 and P2, but not in spatial learning per se as observed during training sessions. Deficits were greater in the early phase

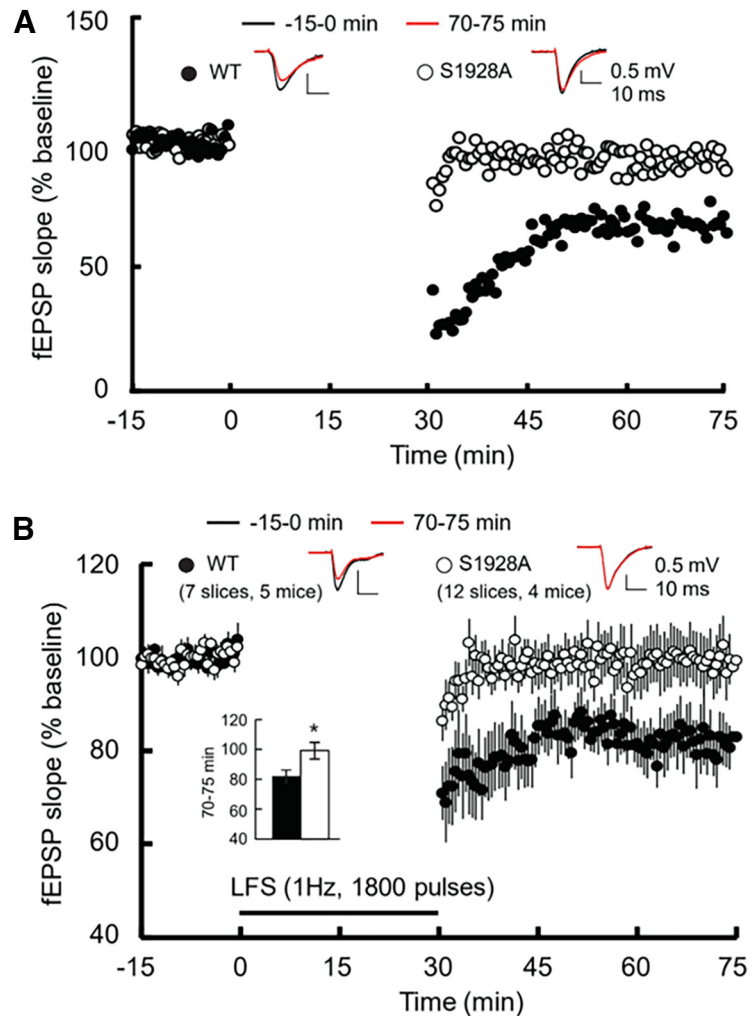


**Figure 7.** S1928A KI mice showed impaired LTD in response to a train of 1-Hz stimuli. Shown are time courses of fEPSP slopes in acute hippocampal slices prepared between 10 A.M. and 12 P.M. from six- to eight-week-old WT and KI mice. Timepoint 0 indicates beginning of 1 Hz, 1800 stimuli regime. Top insets show representative fEPSP traces. **A**, One representative experiment for WT (white circles) and one for S1928A KI mice (black circles). **B**, Means  $\pm$  SEM (vertical lines) from all experiments for WT and KI. Lower left inset: bar plot of the means ( $\pm$ SEM) of the 70- to 75-min bin averages as % of baseline (i.e., bin averages of last 5 min before tetanus). LTD was significant for WT ( $82.2 \pm 7.5\%$  of baseline,  $p < 0.00001$ ) but not S1928A KI ( $99.2 \pm 9.6\%$  of baseline,  $p = 0.51$ ). The difference between genotypes was significant ( $*p < 0.05$ ,  $t$  test). Black bar (bottom) indicates LFS induction protocol time period. Legend (top) shows  $N$  of slices and animals for experiment.

of consolidation of reference memory, but reduced by more training. Once acquired, the memory was remarkably stable in the KI mice; the increases in latencies to reach the goal were minimal comparing the remote memory in P3 with earlier memory in P2, and dwell time in the goal quadrant did not decrease (Fig. 3G,H). In fact, the increase in latency was significantly smaller in KI compared with WT mice ( $p = 0.04$ ), suggesting that the memory is more stable in KI than WT mice (Fig. 3G). There was also a trend in increased goal quadrant dwell time for KI compared with WT mice ( $p = 0.16$ ), although this difference did not reach statistical significance.

#### Reversal of spatial learning in the MWM is strongly affected in S1928A KI mice

Flexibility of consolidated reference memory was tested directly through reversal training, which began  $\sim 24$  h after the P3 test with the platform moved to the opposite side of the pool. Trial latency decreased over the 4 d of training (main effect by Day

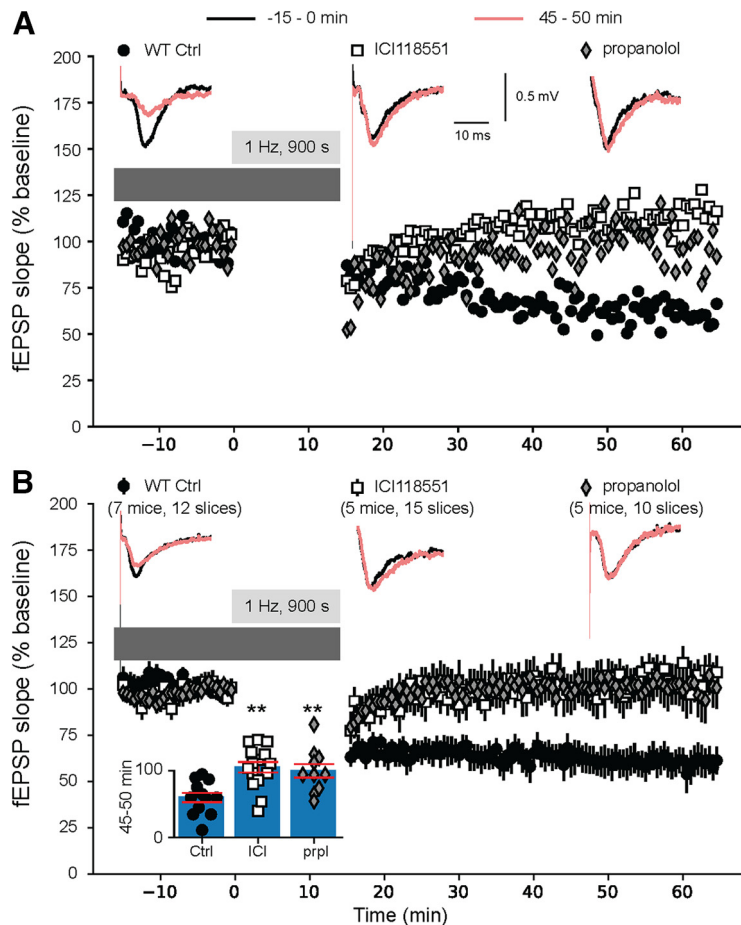


**Figure 8.**  $\beta_2$  AR blockers inhibit LTD. Shown are time courses of fEPSP slopes in acute hippocampal slices prepared between 4 and 6 P.M. from three- to four-month-old WT mice. Timepoint 0 indicates beginning of 1-Hz, 900 stimuli regime. Top insets show representative fEPSP traces. Horizontal dark gray bars indicate time of drug application and light gray bars LFS induction protocol time period. **A**, One representative experiment for vehicle (H<sub>2</sub>O; black circles), propranolol (1  $\mu$ M; gray diamonds) and ICI118551 (10 nM; white squares). **B**, Means  $\pm$  SEM (vertical lines) from all experiments. Lower left inset: bar plot of the means ( $\pm$  SEM) of the 45- to 50-min bin averages as % of baseline (i.e., bin averages of last 5 min before tetanus). LTD was significant for vehicle ( $59.8 \pm 7.3\%$  of baseline,  $p < 0.0002$ ) but not propranolol ( $99.3 \pm 10.2\%$  of baseline,  $p = 0.963$ ) nor ICI118551 ( $105.1 \pm 8.26\%$ ,  $p = 0.544$ ). The differences between drugs versus vehicle were significant (\*\* $p < 0.01$ , ANOVA followed by *post hoc* Tukey's test). Legend (top) shows *N* of slices and animals for experiment.

$p < 0.001$ ; Fig. 6A,B), which did not differ between genotypes (main effect by GT  $p = 0.90$ ; GT  $\times$  Day interaction  $p = 0.80$ ). In the probe test 24 h after the last training session (P4), both genotypes showed a significant preference for the reversal goal quadrant over the others (WT: SW-NE  $p < 0.001$ , SW-NW  $p < 0.001$ , SW-SE  $p < 0.001$ ; KI: S1928A SW-NE  $p < 0.001$ , SW-NW  $p < 0.001$ , SW-SE  $p < 0.001$ ; Fig. 6C). However, KI mice spent significantly less time in the reversal platform quadrant than WT (“SW”;  $p = 0.005$ ) and precise reversal platform location ( $p = 0.003$ ; Fig. 6D,E).

Intriguingly, KI mice displayed a significant preference for the original goal quadrant (“NE”) over the remaining two non-goal quadrants (S1928A NE-NW  $p = 0.0015$ , NE-SE  $p = 0.0085$ ) whereas WT mice did not (WT NE-NW  $p = 0.182$ , NE-SE  $p = 0.822$ ; Fig. 6C, red asterisks). Accordingly, KI mice exhibited significantly greater preference versus WT for the NE quadrant ( $p = 0.008$ ; Fig. 6D). The DI by dwell time in the reversal versus original goal quadrant was also significantly lower in KI versus WT ( $p = 0.009$ ; Fig. 6G). At the same time, S1928A did not

significantly differ in latency to first reach the reversal or original platform location (reversal:  $p = 0.65$ ; original:  $p = 0.84$ ; Fig. 6F), which suggests that KI mice learned the new goal location as well as WT mice.

These findings raise the possibility that S1928A KI mice exhibited less preference for the reversal position in part because of reduced “unlearning” or “forgetting” of the original platform position (Ryan and Frankland, 2022). This effect could be driven by reduced extinction of the consolidated original memory, impaired overriding of the consolidated original memory by the consolidated reversal memory, or both. Impaired extinction of the consolidated original memory is also consistent with the above mentioned finding that latency to reach the platform zone increases less in the KI versus WT mice, when comparing performance between P2 and P3 (Fig. 3G).

The mouse position density heatmap during P4 revealed a hotspot that precisely overlapped with the reversal platform zone for both genotypes (“SW,” bottom left). However, in S1928A mice the hotspot was more diffuse than in WT. In addition, the location heatmap trailed back to the original goal location (“NE,” top right; Fig. 6H), which is again consistent with the possibility of impaired “unlearning” or “forgetting” of the original platform location. These findings suggest that S1928A KI mice retained a stronger memory of the original platform location than WT mice.

### S1928A KI mice are deficient in long-term depression in hippocampal slices

Prior reports suggest that NMDA receptor (NMDAR)-dependent LTD is required for normal reversal of reference memory (Duffy et al., 2008; Dong et al., 2013; Awasthi et al., 2019) and that Ca<sub>v</sub>1.2 is important for LTD (Christie et al., 1997; Coussens et al., 1997; Norris et al., 1998; Zhao and Constantine-Paton, 2007). To test whether the impaired reversal learning in S1928A KI mice could be attributed to impaired LTD, we analyzed LTD in field recordings from acute hippocampal slices. NMDAR-dependent LTD was originally induced by a stimulus train of 1 Hz for 15 min (900 pulses) in rats less than six weeks old (Dudek and Bear, 1992, 1993). However, in animals older than six-week LTD requires a tetanus of 1 Hz for 30 min under standard conditions (Kemp et al., 2000). This LTD is also completely blocked by NMDAR antagonists (Kemp et al., 2000). Thus, we initially used the 1 Hz/30 min protocol to analyze LTD in six- to eight-month-old WT and S1928A KI mice. LTD was determined by comparing the averages of the initial slopes of the field EPSPs (fEPSPs) recorded over the last 5 min before the 1-Hz tetanus (baseline) and those recorded between 70 and 75 min after start of the tetanus. WT mice displayed consistent LTD (82.2% of baseline, SE = 7.5%,  $p < 0.00001$ ) when S1928A KI did not (99.2%, SE = 9.6%,  $p = 0.51$ ; Fig. 7). The normalized averages of the initial slopes of the fEPSPs recorded between 70 and 75 min after start of the 1-Hz stimulus trains were significantly greater for KI than WT mice (effect size = 17.1%, SE = 7.3%,  $p = 0.02$ ; Fig. 7, inset).

The preceding findings are consistent with earlier reports implicating LTD in reversal learning and cognitive flexibility (Duffy et al., 2008; Dong et al., 2013; Awasthi et al., 2019). They suggest the deficit in LTD as a mechanistic underpinning for the deficit in reversal learning of S1928A KI mice. However, the above LTD experiments were performed in six- to eight-month-old mice. Because our behavioral studies were mostly performed in three- to six-month-old mice we expanded our analysis to evaluate LTD in three- to four-month-old mice. Similar to the above LTD, PTT-LTP depends on Ca<sub>v</sub>1.2 and its phosphorylation on Ser<sup>1928</sup> by PKA (Qian et al., 2012, 2017; Patriarchi et al., 2016). When slices are prepared in the morning when rodents are in their inactive phase and sleep, PTT-LTP requires addition of an exogenous  $\beta_2$  AR agonist (M.J. Thomas et al., 1996; Qian et al., 2012, 2017; Patriarchi et al., 2016). However, earlier work suggested that in slices prepared during the active phase PTT-LTP can be induced without addition of a  $\beta_2$  AR agonist (Sarabdjitsingh et al., 2014), which was recently confirmed in a systematic manner (Birnie et al., 2023). Accordingly, it is conceivable that during the active night time phase endogenous supply of the  $\beta_2$  AR agonist norepinephrine (NE) augments phosphorylation of Ca<sub>v</sub>1.2 on Ser<sup>1928</sup> to a level that is sufficient for the induction of LTD.

Consistent with this hypothesis, and quite remarkable, we found that in slices that were prepared around 5 P.M. from three- to four-month-old mice LTD is readily inducible by a 1-Hz/15-min protocol (Fig. 8). This LTD is blocked by propranolol, which blocks all  $\beta$  ARs, and ICI118551, which is a highly selective and highly potent blocker of the  $\beta_2$  AR. The role of specifically the  $\beta_2$  AR–S1928 pathway here (vs general  $\beta_2$  AR signaling) is supported by a final set of experiments in which we find that the synthetic peptide myr-Pep2, which selectively displaces the  $\beta_2$  AR from Ca<sub>v</sub>1.2 (Patriarchi et al., 2016; Qian et al., 2017), also blocks this LTD (Fig. 9). A scrambled version of myr-Pep2 does not affect this LTD. Accordingly, LTD in adult mice requires upregulation of Ca<sub>v</sub>1.2 activity via  $\beta_2$  AR–S1928 signaling.

Our results indicate that phosphorylation of the Ca<sup>2+</sup> channel Ca<sub>v</sub>1.2 on Ser<sup>1928</sup> by PKA augments spatial memory consolidation and plays a critical role in its flexibility. Furthermore, they link these functions to the regulation of synaptic strength through, respectively, PTT-LTP and LTD, both of which depending on phosphorylation of S1928, which is induced by  $\beta_2$  ARs that are linked to Ca<sub>v</sub>1.2 (Patriarchi et al., 2016; Qian et al., 2017; Figs. 7–9). Notably, LTP induced by two brief 100-Hz tetani, which is NMDAR dependent, is perfectly normal in the S1928A KI mice (Fig. 10).

## Discussion

The decrease in habituation in the open field and the reductions in preference for the novel arm in the Y maze and the object in a novel location indicate that elimination of Ser<sup>1928</sup> phosphorylation

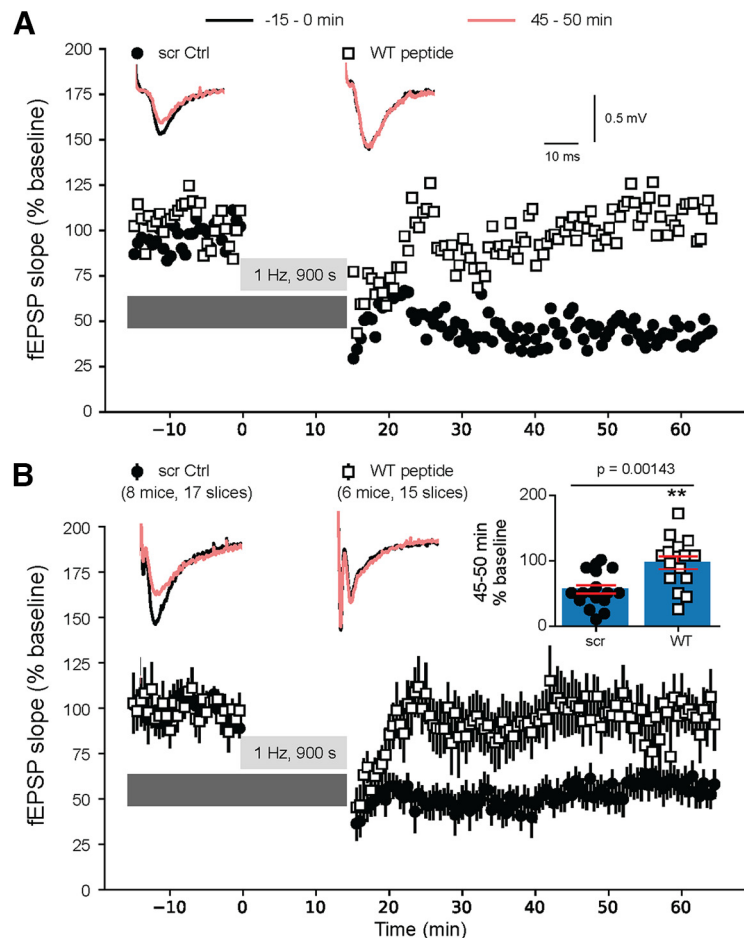


**Figure 9.** Displacement of the  $\beta_2$  AR from Ca<sub>v</sub>1.2 inhibits LTD. Shown are time courses of fEPSP slopes in acute hippocampal slices prepared between 4 and 6 P.M. from three- to four-month-old WT mice. Timepoint 0 indicates beginning of 1-Hz, 900 stimuli regime. Top insets show representative fEPSP traces. Horizontal dark gray bars indicate time of peptide application and light gray bars LFS induction protocol time period. **A**, One representative experiment for scrambled control peptide (scr Ctrl, 10  $\mu$ M myrPep2scr; black circles) and peptide with WT sequence of the binding site for the  $\beta_2$  AR on Ca<sub>v</sub>1.2 (WT peptide, 10  $\mu$ M of myrPep2; white squares). **B**, Means  $\pm$  SEM (vertical lines) from all experiments. Upper right inset, Bar plot of the means ( $\pm$ SEM) of the 45- to 50-min bin averages as % of baseline (i.e., bin averages of last 5 min before tetanus). LTD was significant for control myrPep2scr (56.9  $\pm$  6.5% of baseline,  $p$  = 0.000006) but not WT myrPep2 (98.8  $\pm$  9.9% of baseline,  $p$  = 0.891). The difference between peptides was significant (\*\* $p$  = 0.00143,  $t$  test). Legend (top) shows  $N$  of slices and animals for experiment.

affects spatial memory formation and recall during its early phases. In the MWM probe trials P1 and P2, S1928A KI showed a significantly higher latency to reach the target platform zone versus WT mice. Consistently, times spent in the target quadrant and platform zones were significantly decreased in P1, and such a trend was also seen in P2. However, KI mice did not exhibit a deficit in acquisition of the task as indicated by comparable latencies during the daily training trials in the MWM. Collectively, these results suggest a slower rate of early spatial reference memory consolidation for KI versus WT mice (Vorhees and Williams, 2006). The reduced rate of early consolidation in S1928A KI mice correlates with a loss of PTT-LTP, which strictly depends on signaling by the  $\beta_2$  AR (Qian et al., 2012) and specifically on the upregulation of the activity of Ca<sub>v</sub>1.2 via its phosphorylation on Ser<sup>1928</sup> (Patriarchi et al., 2016; Qian et al., 2017). That these effects are modest is consistent with the finding that S1928 phosphorylation is needed for PTT-LTP (Qian et al., 2017) but not for NMDA receptor-dependent standard LTP induced by two 1-s-long 100-Hz tetani (Fig. 10) and that memory formation is primarily driven by such NMDA receptor-

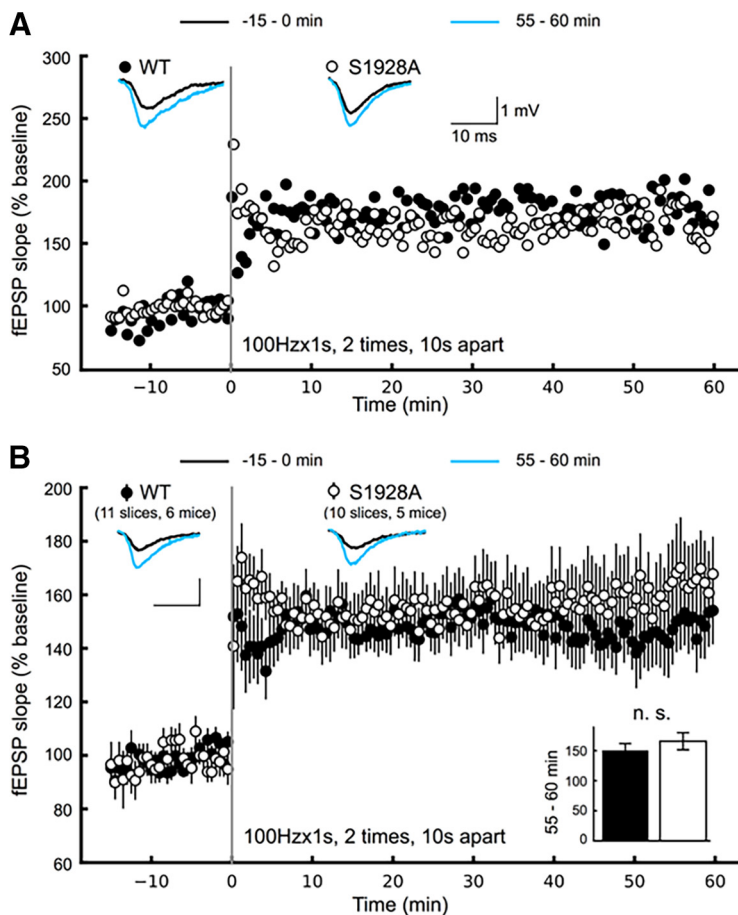


**Figure 10.** S1928A mice showed normal LTP in response to two trains of 100 Hz. Shown are time courses of fEPSP slopes using acute hippocampal slices from two- to three-month-old WT and KI mice prepared between 10 A.M. and 12 P.M. Timepoint 0 marks the first of two 100-Hz tetani, which were each 1 s long and 10 s apart. Top insets show representative fEPSP traces. **A**, One representative experiment for WT (black circles) and one for S1928A KI mice (white circles). **B**, Means  $\pm$  SEM (vertical lines) from all experiments for WT and KI. Lower right inset: bar plot of the means ( $\pm$ SEM) of the 55- to 60-min bin averages as % of baseline (i.e., bin averages of last 5 min before tetanus). LTP was significant for WT ( $141.6 \pm 9.4\%$  of baseline,  $p < 0.00118$ ) as well as S1928A KI ( $160.6 \pm 13.1\%$  of baseline,  $p = 0.00134$ ). The difference between genotypes was not significant (n.s.,  $p = 0.246$ ,  $t$  test). Legend (top) shows  $N$  of slices and animals for experiment.

dependent LTP (Whitlock et al., 2006; Kessels and Malinow, 2009; Morris, 2013; Goto et al., 2021). All these results and considerations are consistent with a role of PTT-LTP or related forms of synaptic plasticity that involve Ca<sup>2+</sup> influx through Ca<sub>v</sub>1.2 in spatial memory and in particular its rate of consolidation.

Signaling by NE is important for the learning process in novel environments that provoke an emotionally salient response (Cahill et al., 1994; Berman and Dudai, 2001; Hu et al., 2007; Minzenberg et al., 2008; Carter et al., 2010) like the survival instinct to escape from water in the MWM. The  $\beta$  AR antagonist propranolol impairs rodent MWM performance in probe tests of consolidated reference memory one or more days after training but not spatial learning during training trials (S.A. Thomas and Palmiter, 1997; Cahill et al., 2000; Czech et al., 2000; Murchison et al., 2004). These effects match remarkably well with our findings that S1928A KI mice are impaired in initial phases of memory formation, but not the immediate learning per se, expanding our rather limited mechanistic understanding of early memory consolidation by  $\beta$  AR signaling. Accordingly, NE could promote consolidation or recall of memory to a significant degree by inducing phosphorylation of Ca<sub>v</sub>1.2 on S1928, thereby

stimulating Ca<sup>2+</sup> influx through this channel (Nystoriak et al., 2017; Qian et al., 2017; Man et al., 2020a).

Recall of remote spatial memory by the S1928A KI mice was at least as good as that of WT mice in the P3 probe trials, which occurred 10 d after the last training on day 7. In fact, the increase in latency to reach the goal location was quite substantial for WT, as expected, but minimal for KI mice. These results suggest that long-term consolidation and maintenance of reference memory was in fact stronger in the KI than WT mice.

Latencies of S1928A KI and WT to reach the platform in reversal training improved at the same rate and were comparable in the P4 probe test. These data suggest that KI and WT mice did not differ in spatial reversal learning during training. However, during P4, KI mice spent significantly less time in the reversal goal quadrant and reversal platform circumference than WT. Strikingly, KI mice also spent a significantly greater proportion of time in the original goal quadrant than WT mice, which explains at least in part the reduced dwell time in the reversal goal zone seen for the KI versus WT mice. This finding is consistent with a slower rate of change or resistance to flexibility of the global spatial reference memory in the MWM. Accordingly, KI mice seemed to be impaired in modification, extinction, or forgetting of the consolidated original memory. This effect was visible throughout 10-s epochs of the P4 test (Fig. 11), where KI mice made more repeated visits to the original goal location throughout the whole duration of the 60-s probe trial.

Prior studies of reversal learning in the MWM have linked deficits in performance, and specifically inappropriate returning to the original platform location, to deficits in NMDAR-dependent LTD (Duffy et al., 2008; Nicholls et al., 2008; Dong et al., 2013; Awasthi et al., 2019). We found that LTD is deficient in S1928A KI mice (Fig. 7).

This finding reveals an impairment in synaptic plasticity for these KI mice within circuitry known to be critical to the expression of learning and memory. Mechanistically, this finding is consistent with earlier studies that showed that LTD depends during its induction on the activity of both, L-type Ca<sup>2+</sup> channels (Christie et al., 1997; Coussens et al., 1997; Norris et al., 1998; Zhao and Constantine-Paton, 2007) and PKA (Lu et al., 2008; Sanderson et al., 2016). We expand this molecular understanding of LTD by providing direct evidence that standard LTD induced by 900 stimuli at 1 Hz also requires a basal activity level of the  $\beta_2$  AR (Fig. 8) as well as a direct association of the  $\beta_2$  AR with Ca<sub>v</sub>1.2 (Fig. 9). The latter finding indicates that this LTD specifically depends on the  $\beta_2$  AR-cAMP/PKA-Ca<sub>v</sub>1.2 signaling pathway. PKA phosphorylates Ser<sup>1928</sup> to augment Ca<sup>2+</sup> influx through Ca<sub>v</sub>1.2 (De Jongh et al., 1996; Davare et al., 1999; Hall et al., 2007; Nystoriak et al., 2017; Qian et al., 2017). This increase in Ca<sup>2+</sup> influx could promote removal of AMPA receptors (AMPA) from postsynaptic sites and their endocytosis, which is required for LTD (Dong et al., 2015; Sanderson et al., 2016; Awasthi et al., 2019). Taken together, these earlier studies and our current findings point toward LTD as a mechanism important for flexibility in reversal learning of a new platform

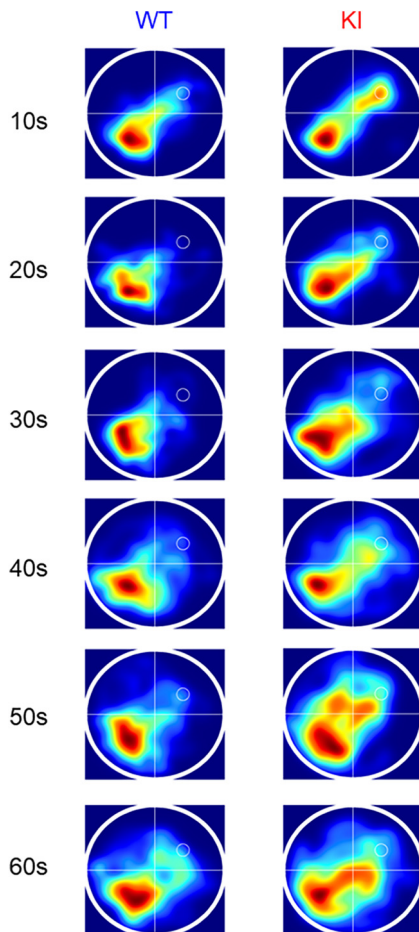


**Figure 11.** S1928A mice showed impaired consolidation of reversal reference memory across time bins, during probe test in the Morris water maze. Position density heatmaps for genotype groups during the early consolidation probe test after reversal training (P4). Maps are arranged from top to bottom as 10-s time bins in series throughout the 60-s probe, and labeled as such. WT are on the left, and KI on the right. Hotter colors (reds) represent greater density of individual positions across each time bin, and cooler colors (blues) represent lesser density.

location in the MWM possibly by contributing to the process of forgetting (Ryan and Frankland, 2022).

### Limitations of the study and perspective

S1928A KI mice are not only impaired in LTD but also PTT-LTP (Qian et al., 2017), which could affect consolidation of the new platform location memory, analogous to that of original platform location seen in P1 and P2. That said, latency to reach the new platform was not affected in the KI mice in P4. However, an effect that is small and not readily detectable in reversal learning cannot be excluded. Thus, it is conceivable that a stronger old memory because of lack of LTD-driven forgetting acted together with some latent impairment of newly formed memory so that KI mice gravitate more strongly to the old location than WT. Finally, the KI mice could also be impaired in potentiation of synapses during reversal learning that would otherwise override the potentiation of synapses that occurred during the formation of the original location memory. Such potentiation can strengthen synaptic circuits that repress other circuits that were potentiated during the preceding learning, which could complement or act as an alternative to extinction mechanisms via LTD (Ryan and Frankland, 2022).

NE- $\beta_2$  AR-Ca<sub>v</sub>1.2 signaling is probably present and important across multiple cortical regions, including those important for consolidation of spatial memory. This regulatory mechanism is likely engaged in the dorsal hippocampus known to be important for spatial memory, where the *ex vivo* recordings of PTT-LTP previously described (Qian et al., 2017) and LTD in this study were performed. It is plausible that this regulatory mechanism is also at work in neocortical areas such as the medial prefrontal cortex (mPFC) and anterior cingulate cortex and in the transfer of information or spatial representations from the hippocampus to these areas for the consolidation of spatial reference memory (Euston et al., 2007; Takehara-Nishiuchi and McNaughton, 2008; Goto et al., 2021). This may help explain the deficits observed in memory consolidation in S1928A KI mice. However, technical limitations dictated the use of global S1928A KI mice. Accordingly, the effects of the S1928A mutation on spatial memory formation cannot be ascribed with certainty to altered PTT-LTP and LTD specifically in the hippocampal CA1 region versus other brain regions. However, this work unequivocally implicates S1928 phosphorylation downstream of NE signaling in spatial learning.

Furthermore, early learning in the MWM was not affected in the S1928A KI mice, implicating that initial learning requires mechanisms other than regulation of Ca<sub>v</sub>1.2 by PKA. This is consistent with the well-established critical roles of Ca<sup>2+</sup> influx through NMDARs and the ensuing activation of CaMKII in multiple stages of memory formation, including early learning phases (Silva et al., 1992; Mayford et al., 1996; Frankland et al., 2001; Morris, 2013; Hell, 2014).

Spatial memory formation was far from being completely compromised in S1928A KI mice. Thus, molecular mechanisms in addition to PKA-mediated Ser<sup>1928</sup> phosphorylation downstream of  $\beta_2$  AR signaling must exist that govern this process. For instance, NE-induced phosphorylation of the GluA1 subunit of AMPARs on Ser<sup>845</sup> had been implicated in promoting early consolidation of context-dependent memory in fear conditioning (Hu et al., 2007). PTT-LTP as well as LTD require phosphorylation of GluA1 on Ser<sup>845</sup> and Ca<sub>v</sub>1.2 on Ser<sup>1928</sup> (Lee et al., 2010; Qian et al., 2012, 2017; Patriarchi et al., 2016). Thus, the intriguing possibility arises that both phosphorylations play roles in spatial learning and reversal learning in the MWM, potentially in conjunction with each other, as AMPAR activity can drive opening of L-type Ca<sup>2+</sup> channels in dendritic spines (Harnett et al., 2012; Beaulieu-Laroche and Harnett, 2018). Such potentially synergistic roles of upregulation of GluA1 and Ca<sub>v</sub>1.2 activity by NE and PKA signaling in synaptic plasticity and memory formation are accordingly ripe for further examination.

NMDAR-dependent LTD induced by a 15-min/1-Hz stimulus paradigm is typically reported in two- to three-week-old rodents but difficult to induce after six weeks of age (Dudek and Bear, 1992, 1993; Kemp et al., 2000). To match the mice's ages of the LTD recordings with that of the behavior analysis we investigated whether we can induce LTD with the standard 1 Hz/15 min protocol in hippocampal slices prepared from three- to four-month-old mice at the beginning of their wake phase (around 5 P.M.) when NE levels rise to augment alertness because that increase in NE could help augment Ca<sub>v</sub>1.2 activity via the  $\beta_2$  AR-S1928 signaling pathway. In fact, under our conditions we readily observed such standard LTD. Analogously, PTT-LTP, which also depends on  $\beta_2$  AR-triggered phosphorylation of S1928, can be induced during rodents' active phases without supplementation with a  $\beta_2$  AR agonist as necessary during inactive phases (Sarabdjitsingh et al., 2014; Birnie et al.,

2023). It is, thus, tempting to speculate that LTD and thereby reversal learning is governed by the circadian rhythm on NE availability. However, there are likely additional circadian mechanisms at work that can affect LTD including circadian changes in the release of the NMDAR co-agonist D-serine from astrocytes (Papouin et al., 2017) and, more generally, synaptic plasticity that is influenced by circadian change in corticosterone levels (Sarabdjitsingh et al., 2014; Birnie et al., 2023). Our findings now provide strong impetus for further work on the circadian role of NE in synaptic plasticity and cognitive flexibility in spatial learning.

In summary, we can now view NE-induced phosphorylation of Ca<sub>v</sub>1.2 at Ser<sup>1928</sup> as an important molecular event in PTT-LTP and LTD in the hippocampus and in the formation and flexibility of spatial memory. Thus, Ser<sup>1928</sup> phosphorylation may be of general importance for modulating and fine-tuning plasticity in neural circuits relevant to learning and memory. Further functional analysis of Ser<sup>1928</sup> phosphorylation could ultimately shine light on how altered expression or functioning of Ca<sub>v</sub>1.2 because of variation and mutation in the *CACNA1C* gene interacts with NE signaling to affect brain functions and behavior in both health and neuropsychiatric disorders.

## References

- Awasthi A, Ramachandran B, Ahmed S, Benito E, Shinoda Y, Nitzan N, Heukamp A, Rannio S, Martens H, Barth J, Burk K, Wang YT, Fischer A, Dean C (2019) Synaptotagmin-3 drives AMPA receptor endocytosis, depression of synapse strength, and forgetting. *Science* 363:eav1483.
- Balijepalli RC, Foell JD, Hall DD, Hell JW, Kamp TJ (2006) Localization of cardiac L-type Ca(2+) channels to a caveolar macromolecular signaling complex is required for beta(2)-adrenergic regulation. *Proc Natl Acad Sci U S A* 103:7500–7505.
- Beaulieu-Laroche L, Harnett MT (2018) Dendritic spines prevent synaptic voltage clamp. *Neuron* 97:75–82.e3.
- Berman DE, Dudai Y (2001) Memory extinction, learning anew, and learning the new: dissociations in the molecular machinery of learning in cortex. *Science* 291:2417–2419.
- Bhat S, Dao DT, Terrillion CE, Arad M, Smith RJ, Soldatov NM, Gould TD (2012) *CACNA1C* (Cav1.2) in the pathophysiology of psychiatric disease. *Prog Neurobiol* 99:1–14.
- Birnie MT, Claydon MDB, Troy O, Flynn BP, Yoshimura M, Kershaw YM, Zhao Z, Demski-Allen RCR, Barker GRI, Warburton EC, Bortolotto ZA, Lightman SL, Conway-Campbell BL (2023) Circadian regulation of hippocampal function is disrupted with corticosteroid treatment. *Proc Natl Acad Sci U S A* 120:e2211996120.
- Cahill L, Prins B, Weber M, McGaugh JL (1994) Beta-adrenergic activation and memory for emotional events. *Nature* 371:702–704.
- Cahill L, Pham CA, Setlow B (2000) Impaired memory consolidation in rats produced with beta-adrenergic blockade. *Neurobiol Learn Mem* 74:259–266.
- Caron MG, Lefkowitz RJ (1993) Catecholamine receptors: structure, function and regulation. *Recent Prog Horm Res* 277–290.
- Carter ME, Yizhar O, Chikahisa S, Nguyen H, Adamantidis A, Nishino S, Deisseroth K, de Lecea L (2010) Tuning arousal with optogenetic modulation of locus coeruleus neurons. *Nat Neurosci* 13:1526–1533.
- Choi JH, Sim SE, Kim JI, Choi DI, Oh J, Ye S, Lee J, Kim T, Ko HG, Lim CS, Kaang BK (2018) Interregional synaptic maps among engram cells underlie memory formation. *Science* 360:430–435.
- Christie BR, Schexnayder LK, Johnston D (1997) Contribution of voltage-gated Ca<sup>2+</sup> channels to homosynaptic long-term depression in the CA1 region in vitro. *J Neurophysiol* 77:1651–1655.
- Collingridge GL, Peineau S, Howland JG, Wang YT (2010) Long-term depression in the CNS. *Nat Rev Neurosci* 11:459–473.
- Coussens CM, Kerr DS, Abraham WC (1997) Glucocorticoid receptor activation lowers the threshold for NMDA-receptor-dependent homosynaptic long-term depression in the hippocampus through activation of voltage-dependent calcium channels. *J Neurophysiol* 78:1–9.
- Czech DA, Nielson KA, Laubmeier KK (2000) Chronic propranolol induces deficits in retention but not acquisition performance in the water maze in mice. *Neurobiol Learn Mem* 74:17–26.
- Davare MA, Dong F, Rubin CS, Hell JW (1999) The A-kinase anchor protein MAP2B and cAMP-dependent protein kinase are associated with class C L-type calcium channels in neurons. *J Biol Chem* 274:30280–30287.
- Davare MA, Avdonin V, Hall DD, Peden EM, Burette A, Weinberg RJ, Horne MC, Hoshi T, Hell JW (2001) A beta2 adrenergic receptor signaling complex assembled with the Ca<sup>2+</sup> channel Cav1.2. *Science* [Erratum (2001) 293:804] 293:98–101.
- De Jongh KS, Murphy BJ, Colvin AA, Hell JW, Takahashi M, Catterall WA (1996) Specific phosphorylation of a site in the full length form of the alpha 1 subunit of the cardiac L-type calcium channel by adenosine 3',5'-cyclic monophosphate-dependent protein kinase. *Biochem* 35:10392–10402.
- Dong Z, Bai Y, Wu X, Li H, Gong B, Howland JG, Huang Y, He W, Li T, Wang YT (2013) Hippocampal long-term depression mediates spatial reversal learning in the Morris water maze. *Neuropharmacology* 64:65–73.
- Dong Z, Han H, Li H, Bai Y, Wang W, Tu M, Peng Y, Zhou L, He W, Wu X, Tan T, Liu M, Wu X, Zhou W, Jin W, Zhang S, Sacktor TC, Li T, Song W, Wang YT (2015) Long-term potentiation decay and memory loss are mediated by AMPAR endocytosis. *J Clin Invest* 125:234–247.
- Dudek SM, Bear MF (1992) Homosynaptic long-term depression in area CA1 of hippocampus and effects of N-methyl-D-aspartate receptor blockade. *Proc Natl Acad Sci U S A* 89:4363–4367.
- Dudek SM, Bear MF (1993) Bidirectional long-term modification of synaptic effectiveness in the adult and immature hippocampus. *J Neurosci* 13:2910–2918.
- Duffy S, Labrie V, Roder JC (2008) D-serine augments NMDA-NR2B receptor-dependent hippocampal long-term depression and spatial reversal learning. *Neuropsychopharmacology* 33:1004–1018.
- Euston DR, Tatsuno M, McNaughton BL (2007) Fast-forward playback of recent memory sequences in prefrontal cortex during sleep. *Science* 318:1147–1150.
- Ferreira MA, et al. (2008) Collaborative genome-wide association analysis supports a role for ANK3 and CACNA1C in bipolar disorder. *Nat Genet* 40:1056–1058.
- Frankland PW, O'Brien C, Ohno M, Kirkwood A, Silva AJ (2001) Alpha-CaMKII-dependent plasticity in the cortex is required for permanent memory. *Nature* 411:309–313.
- Goto A, Bota A, Miya K, Wang J, Tsukamoto S, Jiang X, Hirai D, Murayama M, Matsuda T, McHugh TJ, Nagai T, Hayashi Y (2021) Stepwise synaptic plasticity events drive the early phase of memory consolidation. *Science* 374:857–863.
- Grailhe R, Waeber C, Dulawa SC, Hornung JP, Zhuang X, Brunner D, Geyer MA, Hen R (1999) Increased exploratory activity and altered response to LSD in mice lacking the 5-HT(5A) receptor. *Neuron* 22:581–591.
- Green EK, Grozeva D, Jones I, Jones L, Kirov G, Caesar S, Gordon-Smith K, Fraser C, Forty L, Russell E, Hamshere ML, Moskva V, Nikolov I, Farmer A, McGuffin P Wellcome Trust Case Control Consortium; Holmans PA, Owen MJ, O'Donovan MC, Craddock N (2010) The bipolar disorder risk allele at CACNA1C also confers risk of recurrent major depression and of schizophrenia. *Mol Psychiatry* 15:1016–1022.
- Grover LM, Teyler TJ (1990) Two components of long-term potentiation induced by different patterns of afferent activation. *Nature* 347:477–479.
- Hall DD, Davare MA, Shi M, Allen ML, Weisenhaus M, McKnight GS, Hell JW (2007) Critical role of cAMP-dependent protein kinase anchoring to the L-type calcium channel Cav1.2 via A-kinase anchor protein 150 in neurons. *Biochemistry* 46:1635–1646.
- Halt AR, Dallapiazza R, Yu H, Stein IS, Qian H, Junti S, Wojcik S, Brose N, Sliva A, Hell JW (2012) CaMKII binding to GluN2B is critical during memory consolidation. *EMBO J* 31:1203–1216.
- Harnett MT, Makara JK, Spruston N, Kath WL, Magee JC (2012) Synaptic amplification by dendritic spines enhances input cooperativity. *Nature* 491:599–602.
- Hell JW (2014) CaMKII: claiming center stage in postsynaptic function and organization. *Neuron* 81:249–265.
- Hell JW, Westenbroek RE, Warner C, Ahljianian MK, Prystay W, Gilbert MM, Snutch TP, Catterall WA (1993) Identification and differential subcellular localization of the neuronal class C and class D L-type calcium channel alpha 1 subunits. *J Cell Biol* 123:949–962.

- Hell JW, Westenbroek RE, Breeze LJ, Wang KKW, Chavkin C, Catterall WA (1996) N-methyl-D-aspartate receptor-induced proteolytic conversion of postsynaptic class C L-type calcium channels in hippocampal neurons. *Proc Natl Acad Sci U S A* 93:3362–3367.
- Hu H, Real E, Takamiya K, Kang MG, Ledoux J, Haganir RL, Malinow R (2007) Emotion enhances learning via norepinephrine regulation of AMPA-receptor trafficking. *Cell* 131:160–173.
- Hulme JT, Lin TW, Westenbroek RE, Scheuer T, Catterall WA (2003) Beta-adrenergic regulation requires direct anchoring of PKA to cardiac CaV1.2 channels via a leucine zipper interaction with A kinase-anchoring protein 15. *Proc Natl Acad Sci U S A* 100:13093–13098.
- Jensen O, Lisman JE (2005) Hippocampal sequence-encoding driven by a cortical multi-item working memory buffer. *Trends Neurosci* 28:67–72.
- Kemp N, McQueen J, Faulkes S, Bashir ZI (2000) Different forms of LTD in the CA1 region of the hippocampus: role of age and stimulus protocol. *Eur J Neurosci* 12:360–366.
- Kessels HW, Malinow R (2009) Synaptic AMPA receptor plasticity and behavior. *Neuron* 61:340–350.
- Krauter AK, Guest PC, Sarnyai Z (2019) The Y-maze for assessment of spatial working and reference memory in mice. *Methods Mol Biol* 1916:105–111.
- Lee HK, Takamiya K, He K, Song L, Haganir RL (2010) Specific roles of AMPA receptor subunit GluR1 (GluA1) phosphorylation sites in regulating synaptic plasticity in the CA1 region of hippocampus. *J Neurophysiol* 103:479–489.
- Lemke T, Welling A, Christel CJ, Blaich A, Bernhard D, Lenhardt P, Hofmann F, Moosmang S (2008) Unchanged beta-adrenergic stimulation of cardiac L-type calcium channels in Ca v 1.2 phosphorylation site S1928A mutant mice. *J Biol Chem* 283:34738–34744.
- Liu G, Papa A, Katchman AN, Zakharov SI, Roybal D, Hennessey JA, Kushner J, Yang L, Chen BX, Kushnir A, Dangas K, Gygi SP, Pitt GS, Colecraft HM, Ben-Johny M, Kalocsay M, Marx SO (2020) Mechanism of adrenergic CaV1.2 stimulation revealed by proximity proteomics. *Nature* 577:695–700.
- Lu Y, Zhang M, Lim IA, Hall DD, Allen ML, Medvedeva Y, McKnight GS, Usachev YM, Hell JW (2008) AKAP150-anchored PKA activity is important for LTD during its induction phase. *J Physiol* 586:4155–4164.
- Malleret G, Hen R, Guillou JL, Segu L, Buhot MC (1999) 5-HT1B receptor knock-out mice exhibit increased exploratory activity and enhanced spatial memory performance in the Morris water maze. *J Neurosci* 19:6157–6168.
- Man KNM, Bartels P, Horne MC, Hell JW (2020a) Tissue-specific adrenergic regulation of the L-type Ca(2+) channel Ca(V)1.2. *Sci Signal* 13:eabc6438.
- Man KNM, Navedo MF, Horne MC, Hell JW (2020b)  $\beta$ 2 Adrenergic receptor complexes with the L-type Ca<sup>2+</sup> channel Ca<sub>v</sub>1.2 and AMPA-type glutamate receptors: paradigms for pharmacological targeting of protein interactions. *Annu Rev Pharmacol Toxicol* 60:155–174.
- Marshall MR, Clark JP 3rd, Westenbroek R, Yu FH, Scheuer T, Catterall WA (2011) Functional roles of a C-terminal signaling complex of CaV1 channels and A-kinase anchoring protein 15 in brain neurons. *J Biol Chem* 286:12627–12639.
- Mayford M, Bach ME, Huang YY, Wang L, Hawkins RD, Kandel ER (1996) Control of memory formation through regulated expression of a CaMKII transgene. *Science* 274:1678–1683.
- Minzenberg MJ, Watrous AJ, Yoon JH, Ursu S, Carter CS (2008) Modafinil shifts human locus coeruleus to low-tonic, high-phasic activity during functional MRI. *Science* 322:1700–1702.
- Mizuseki K, Sirota A, Pastalkova E, Buzsáki G (2009) Theta oscillations provide temporal windows for local circuit computation in the entorhinal-hippocampal loop. *Neuron* 64:267–280.
- Moosmang S, Haider N, Klugbauer N, Adelsberger H, Langwieser N, Müller J, Stiess M, Marais E, Schulla V, Lacinova L, Goebbels S, Nave KA, Storm DR, Hofmann F, Kleppisch T (2005) Role of hippocampal Cav1.2 Ca<sup>2+</sup> channels in NMDA receptor-independent synaptic plasticity and spatial memory. *J Neurosci* 25:9883–9892.
- Morris R (1984) Developments of a water-maze procedure for studying spatial learning in the rat. *J Neurosci Methods* 11:47–60.
- Morris RG (2013) NMDA receptors and memory encoding. *Neuropharmacology* 74:32–40.
- Moser EI, Krobot KA, Moser M-B, Morris RGM (1998) Impaired spatial learning after saturation of long-term potentiation. *Science* 281:2038–2042.
- Murchison CF, Zhang XY, Zhang WP, Ouyang M, Lee A, Thomas SA (2004) A distinct role for norepinephrine in memory retrieval. *Cell* 117:131–143.
- Murphy JG, Sanderson JL, Gorski JA, Scott JD, Catterall WA, Sather WA, Dell'Acqua ML (2014) AKAP-anchored PKA maintains neuronal L-type calcium channel activity and NFAT transcriptional signaling. *Cell Rep* 7:1577–1588.
- Nabavi S, Fox R, Alfonso S, Aow J, Malinow R (2014) GluA1 trafficking and metabotropic NMDA: addressing results from other laboratories inconsistent with ours. *Philos Trans R Soc Lond B Biol Sci* 369:20130145.
- Neves G, Cooke SF, Bliss TV (2008) Synaptic plasticity, memory and the hippocampus: a neural network approach to causality. *Nat Rev Neurosci* 9:65–75.
- Nicholls RE, Alarcon JM, Malleret G, Carroll RC, Grody M, Vronskaya S, Kandel ER (2008) Transgenic mice lacking NMDAR-dependent LTD exhibit deficits in behavioral flexibility. *Neuron* 58:104–117.
- Nichols CB, Rossow CF, Navedo MF, Westenbroek RE, Catterall WA, Santana LF, McKnight GS (2010) Sympathetic stimulation of adult cardiomyocytes requires association of AKAP5 with a subpopulation of L-type calcium channels. *Circ Res* 107:747–756.
- Norris CM, Halpain S, Foster TC (1998) Reversal of age-related alterations in synaptic plasticity by blockade of L-type Ca<sup>2+</sup> channels. *J Neurosci* 18:3171–3179.
- Nygaard M, Demontis D, Foldager L, Hedemand A, Flint TJ, Sørensen KM, Andersen PS, Nordentoft M, Werge T, Pedersen CB, Hougaard DM, Mortensen PB, Mors O, Børglum AD (2010) CACNA1C (rs1006737) is associated with schizophrenia. *Mol Psychiatry* 15:119–121.
- Nystoriak MA, Nieves-Cintrón M, Patriarchi T, Buonarati OR, Prada MP, Morotti S, Grandi E, Fernandes JD, Forbush K, Hofmann F, Sasse KC, Scott JD, Ward SM, Hell JW, Navedo MF (2017) Ser1928 phosphorylation by PKA stimulates the L-type Ca<sup>2+</sup> channel CaV1.2 and vasoconstriction during acute hyperglycemia and diabetes. *Sci Signal* 10:eaf9647.
- Oliveria SF, Dell'Acqua ML, Sather WA (2007) AKAP79/150 anchoring of calcineurin controls neuronal L-type Ca(2+) channel activity and nuclear signaling. *Neuron* 55:261–275.
- Papouin T, Dunphy JM, Tolman M, Dineley KT, Haydon PG (2017) Septal cholinergic neuromodulation tunes the astrocyte-dependent gating of hippocampal NMDA receptors to wakefulness. *Neuron* 94:840–854.e7.
- Patriarchi T, Qian H, Di Biase V, Malik ZA, Chowdhury D, Price JL, Hammes EA, Buonarati OR, Westenbroek RE, Catterall WA, Hofmann F, Xiang YK, Murphy GG, Chen CY, Navedo MF, Hell JW (2016) Phosphorylation of Cav1.2 on S1928 uncouples the L-type Ca<sup>2+</sup> channel from the  $\beta$ 2 adrenergic receptor. *EMBO J* 35:1330–1345.
- Qian H, Matt L, Zhang M, Nguyen M, Patriarchi T, Koval ON, Anderson ME, He K, Lee HK, Hell JW (2012)  $\beta$ 2 adrenergic receptor supports prolonged theta tetanus-induced LTP. *J Neurophysiol* 107:2703–2712.
- Qian H, Patriarchi T, Price JL, Matt L, Lee B, Nieves-Cintrón M, Buonarati OR, Chowdhury D, Nanou E, Nystoriak MA, Catterall WA, Poomvanicha M, Hofmann F, Navedo MF, Hell JW (2017) Phosphorylation of Ser1928 mediates the enhanced activity of the L-type Ca<sup>2+</sup> channel Cav1.2 by the  $\beta$ 2-adrenergic receptor in neurons. *Sci Signal* 10:eaf9659.
- Rumpel S, LeDoux J, Zador A, Malinow R (2005) Postsynaptic receptor trafficking underlying a form of associative learning. *Science* 308:83–88.
- Ryan TJ, Frankland PW (2022) Forgetting as a form of adaptive engram cell plasticity. *Nat Rev* 23:173–186.
- Sanderson JL, Gorski JA, Dell'Acqua ML (2016) NMDA receptor-dependent LTD requires transient synaptic incorporation of Ca<sup>2+</sup>-permeable AMPARs mediated by AKAP150-anchored PKA and calcineurin. *Neuron* 89:1000–1015.
- Sarabdjitsingh RA, Jezequel J, Pasricha N, Mikasova L, Kerkhofs A, Karst H, Groc L, Joëls M (2014) Ultradian corticosterone pulses balance glutamatergic transmission and synaptic plasticity. *Proc Natl Acad Sci USA* 111:14265–14270.
- Silva AJ, Paylor R, Wehner JM, Tonegawa S (1992) Impaired spatial learning in alpha-calcium-calmodulin kinase II mutant mice. *Science* 257:206–211.
- Sinnesger-Brauns MJ, Hetzenauer A, Huber IG, Renström E, Wietzorrek G, Berjukov S, Cavalli M, Walter D, Koschak A, Waldschütz R, Hering S, Bova S, Rorsman P, Pongs O, Singewald N, Striessnig J (2004) Isoform-specific regulation of mood behavior and pancreatic beta cell and

- cardiovascular function by L-type Ca<sup>2+</sup> channels. *J Clin Invest* 113:1430–1439.
- Splawski I, Timothy KW, Sharpe LM, Decher N, Kumar P, Bloise R, Napolitano C, Schwartz PJ, Joseph RM, Condouris K, Tager-Flusberg H, Priori SG, Sanguinetti MC, Keating MT (2004) Ca(V)1.2 calcium channel dysfunction causes a multisystem disorder including arrhythmia and autism. *Cell* 119:19–31.
- Takehara-Nishiuchi K, McNaughton BL (2008) Spontaneous changes of neocortical code for associative memory during consolidation. *Science* 322:960–963.
- Thomas MJ, Moody TD, Makhinson M, O'Dell TJ (1996) Activity-dependent beta-adrenergic modulation of low frequency stimulation induced LTP in the hippocampal CA1 region. *Neuron* 17:475–482.
- Thomas SA, Palmiter RD (1997) Disruption of the dopamine beta-hydroxylase gene in mice suggests roles for norepinephrine in motor function, learning, and memory. *Behav Neurosci* 111:579–589.
- Vorhees CV, Williams MT (2006) Morris water maze: procedures for assessing spatial and related forms of learning and memory. *Nat Protoc* 1:848–858.
- White JA, McKinney BC, John MC, Powers PA, Kamp TJ, Murphy GG (2008) Conditional forebrain deletion of the L-type calcium channel Ca<sub>v</sub>1.2 disrupts remote spatial memories in mice. *Learn Mem* 15:1–5.
- Whitlock JR, Heynen AJ, Shuler MG, Bear MF (2006) Learning induces long-term potentiation in the hippocampus. *Science* 313:1093–1097.
- Zhao JP, Constantine-Paton M (2007) NR2A<sup>-/-</sup> mice lack long-term potentiation but retain NMDA receptor and L-type Ca<sup>2+</sup> channel-dependent long-term depression in the juvenile superior colliculus. *J Neurosci* 27:13649–13654.
- Zhuang X, Oosting RS, Jones SR, Gainetdinov RR, Miller GW, Caron MG, Hen R (2001) Hyperactivity and impaired response habituation in hyperdopaminergic mice. *Proc Natl Acad Sci U S A* 98:1982–1987.